ISTANBUL TECHNICAL UNIVERSITY ★ EURASIA INSTITUTE OF EARTH SCIENCES

CLIMATE IMPACTS OF GAP ON SOUTHEAST ANATOLIA REGION

M.Sc. Thesis by

Sait Altuğ EKİCİ, B.Sc.

Department: **Climate and Marine Sciences**

Programme: **Earth System Science**

JUNE 2008

ISTANBUL TECHNICAL UNIVERSITY ★ EURASIA INSTITUTE OF EARTH SCIENCES

CLIMATE IMPACTS OF GAP ON SOUTHEAST ANATOLIA REGION

M.Sc. Thesis by
Sait Altuğ EKİCİ, B.Sc.
(601061002)

Date of submission : **5 May 2008**

Date of defence examination : **9 June 2008**

Supervisor (Chairman): **Prof. Dr. Mehmet KARACA**
Assoc. Prof. Dr. Ömer Lütfi ŞEN

Members of the Examining Committee: **Prof.Dr. Nüzhet DALFES**

Assoc. Prof.Dr. Sibel MENTEŞ

Assoc. Prof.Dr. Ercan KAHYA

JUNE 2008

İSTANBUL TEKNİK ÜNİVERSİTESİ ★ AVRASYA YER BİLİMLERİ ENSTİTÜSÜ

GAP'IN GÜNEYDOĞU ANADOLU BÖLGESİ'NE İKLİMSEL ETKİLERİ

YÜKSEK LİSANS TEZİ

Sait Altuğ EKİCİ
Bilgisayar Mühendisi
(601061002)

Tezin Enstitüye Verildiği Tarih : 5 Mayıs 2008

Tezin Savunulduğu Tarih : 9 Haziran 2008

Tez Danışmanı : **Prof. Dr. Mehmet KARACA**
Doç. Dr. Ömer Lütfi ŞEN

Diğer Jüri Üyeleri: **Prof.Dr. Nüzhet DALFES**

Doç.Dr. Sibel MENTEŞ

Doç.Dr. Ercan KAHYA

HAZİRAN 2008

ACKNOWLEDGMENTS

I would like to thank my supervisor Prof. Dr. Mehmet Karaca for his contributions and motivations during my study. I also like to express my high gratitude to Assoc. Prof. Dr. Ömer Lütfi Şen for all the help and guidance he has provided for me throughout my studies. I should acknowledge all my colleagues who contributed to this work by their support and ideas.

I feel so grateful to my parents for their emotional supports and especially to my dearest cousin Gül for her priceless helps and sincere encouragements all these years.

Lastly I should express my deepest gratitude to TÜBİTAK for the financial support they had provided me and helping me finish this study without any problems.

May 2008 Altuğ Ekici

CONTENTS

ABBREVIATIONS

BATS	: Biosphere Atmosphere Transfer Scheme
CCSM	: Community Climate System Model
GCM	: General Circulation Model
LAM	: Limited Area Model
NCAR	: National Center for Atmospheric Research
CLM	: Community Land Model
GAP	: Güneydoğu Anadolu Projesi
SiB	: Simple Biosphere Model
CAM	: Community Atmosphere Model

TABLE LIST

Page No.

FIGURE LIST

ABSTRACT

Southeast Anatolia region of Turkey is undergoing an immense change since the Southeast Anatolia Project (GAP) has started in 1980s. With the irrigation activities and new crop cultivations over large areas of land, the region is experiencing a significant land cover change. It was mostly barren, rain-fed areas before the GAP, and now the area is covered with multiple crops and busy farming processes. In order to examine and understand the climate impacts of this land cover change over the region, one year long meteorological observations are performed and a land surface model is run. Automatic weather stations and eddy covariance systems are used for the observational studies. Meteolorological data are gathered from two different sites representing before GAP and after GAP conditions. In this thesis titled as *"Climate Impacts of GAP on Southeast Anatolia Region",* gathered data from September 2006 to August 2007, and the simulation results of Community Land Model (CLM) v.3.0 revealed the current differences in the weather and climate of the region. It is understood that the vegetation cover over irrigated lands, has a cooling effect on the overlying air and it also increases the humidity ratio comparing to the non-irrigated sites. Land surface modeling is performed quite succesfully over southeast Anatolia region and all the simulation results with the observational results are represented in this paper.

ÖZET

1980'lerde Güneydoğu Anadolu Projesi (GAP) başladığından beri, Türkiye'nin Güneydoğu Anadolu Bölgesi büyük bir değişim geçirmektedir. Sulama çalışmaları ve çok geniş arazilerde yeni ürün yetiştirme çabalarıyla, bölge yüzey örtüsü büyük bir değişim yaşamaktadır. GAP'tan önce yağmurla sulanan, çoğunlukla çorak olan bu araziler şimdi farklı ürünler ve yoğun tarım çalışmalarıyla kaplı bulunmakta. Bu yüzey değişimlerinin bölge iklime etkilerini araştırmak ve anlamak için bir yıl boyunca meteorolojik ölçümler yapıldı ve bir yüzey modeli çalıştırıldı. Ölçümsel çalışmalarda GAP öncesi ve sonrasını yansutan iki alanda otomatik meteoroloji istasyonları ve eddy kovaryans sistemleri kullanıldı. *"GAP'ın Güneydoğu Anadolu Bölgesi'ne İklimsel Etkileri" adlı tezde,* eylül 2006'dan Ağustos 2007'ye kadar ölçülen değerler ve Community Land Model (CLM) v.3.0 model simulasyonlarının sonucunda bölge iklimindeki değişiklikler ortaya kondu. Bitki örtüsünün ortamda serinletici bir etkisi olduğu ve aynı zamanda sulanmayan arazilere göre sulanan arazilerde havadaki nemi artırdığı anlaşılmıştır. Güneydoğu Anadolu Bölgesi için yüzey modeli çalışmaları da başarıyla tamamlanmış ve bütün simulasyon sonuçları, gözlem sonuçlarıyla beraber bu çalışmada sunulmuştur.

1. INTRODUCTION

1.1. Goal of the paper

Today the northern plains of ancient Mesopotamia lies in the borders of southeastern Turkey. Being the least developed region of the country, southeast Anatolia region is home to 6,604,205 people and covers 75,358 square kilometer area. In order to improve the life standards of the population and to ensure socioeconomic development of the region, Turkish Government has initiated a vast irrigation project here, Southeastern Anatolia Project, widely known with Turkish initials GAP. Having completed 20% of the project, some parts of the region are now enjoying the irrigation process after so many years. But is it really feasible to irrigate the land and create a desirable site? Or are there some unexpected future outcomes that can cause more harm than good?

To understand the natural activities, and predict the future responses of our environment, it is crucial to evaluate the long term climate characteristics. From the beginning of climate predictions, it is a well known fact that atmospheric mechanisms are closely related to land surface processes. Land surface plays an important role for regulating the surface energy balances and providing evapotranspiration for the atmosphere. Thus different types of land surfaces have a changing influence on these mechanisms. One should consider the atmospheric responses when there is an ongoing land surface change.

As being one of the biggest and most important irrigation projects in the world, the Southeastern Anatolia Project (GAP) is definitely changing the landscape. From semi-arid conditions, new green fields are emerging due to irrigation and immense agricultural activities. These mentioned changes will sure affect the climate over this region. So it is one important question that what are the impacts of irrigation induced cultivation and land cover change on weather and climate of this region. Thus this study aims to seek answer to this question by performing an observational experiment and model simulations.

1.2. Background information on GAP

In the southeastern Anatolia region, the recognition of the water potentials of the Euphrates and Tigris rivers resulted in ideas for GAP (Ünver, 1997). The desired achievements of the project were to produce sustainable development for irrigation and hydropower generation. This water resource project was later transformed into an integrated multi-sectoral regional development program (Ünver, 1997).

Figure.1.1 Map of southeast Turkey

As seen in the Figure.1.1, GAP covers all southeast Anatolia region and 9 provinces namely: Kilis, Gaziantep, Adıyaman, Şanlıurfa, Diyarbakır, Batman, Mardin, Şırnak, and Siirt (Figure.1.2). Construction of dams and industrial developments are focused near the banks of Euphrates and Tigris river basins in this region.

Figure.1.2 Provinces covered in GAP

In historical evolution, ideas of using water resources in this area started with Atatürk, founder of Turkish Republic, around 1930s (T.C. Başbakanlık). After 1980, ongoing projects were all combined under the name of GAP. Since then the project has been enlarged from a single water resource management plan to a socioeconomic sustainable development system.

The main objectives of GAP include elimination of inter-regional development disparities by focusing more investments on southeast Anatolia region, increasing life standards of the population, and providing a sustainable wealth to the Turkish Republic in future.

The concept of GAP should be taken as a regional development project covering the stipulated dam constructions over Euphrates and Tigris, hydroelectrical power plants, irrigation systems, urban and rural infrastructures, industry, education, health, housing, tourism and investments in other sectors (T.C. Başbakanlık).

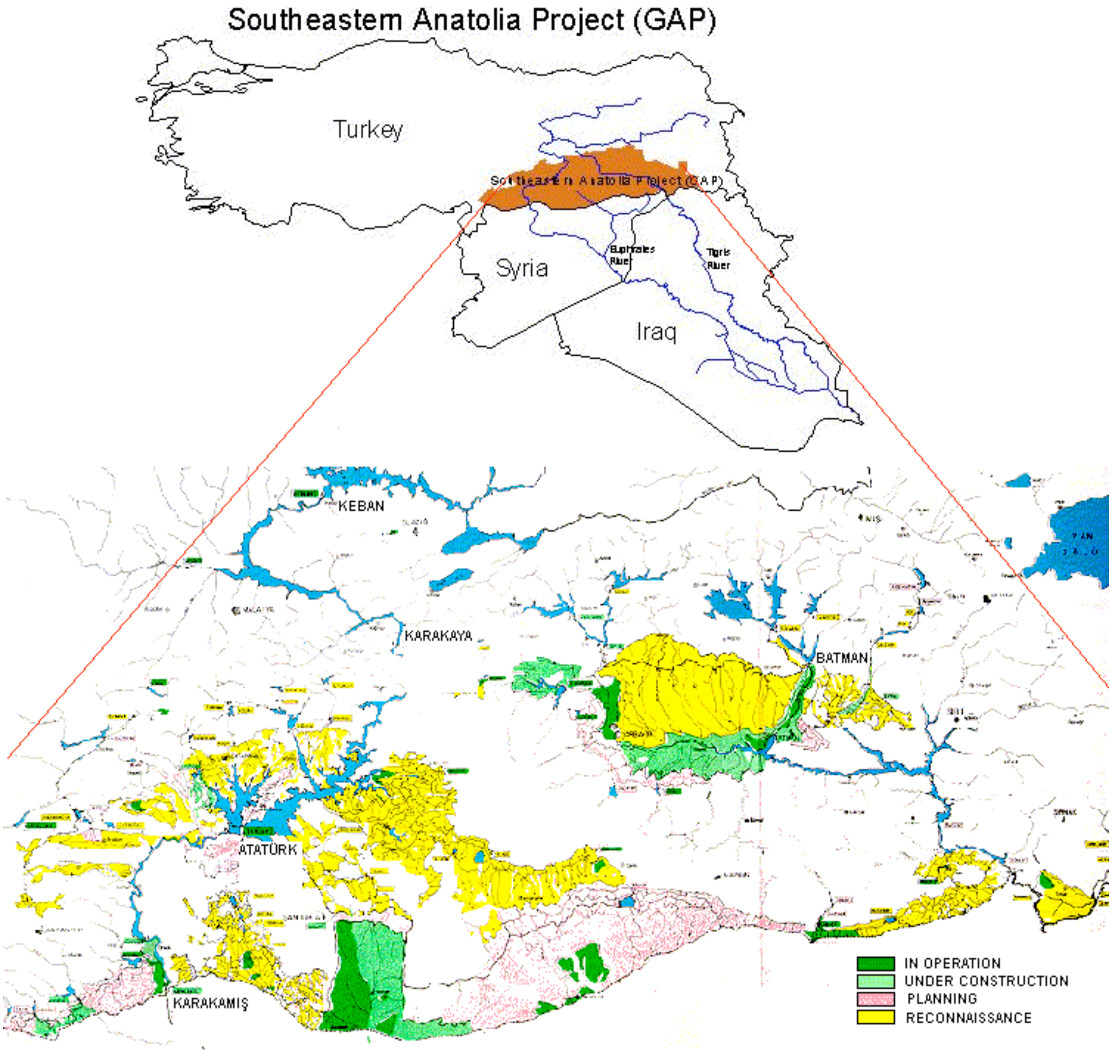

Figure.1.3 Geographical representation of GAP (USDA-FAS, 2007)

When it is completed, GAP will provide 28% of water potential for Turkey, irrigation of 1.7 million hectares (Figure.1.3), over 7476 megawatts of energy which is annually 27 billion kilowatt hours of electricity. It will increase the income level of the region over 5 times and will provide employment to 3.8 million of the population.

The predicted budget of the project is nearly 32 billion US dollars, which makes it the Turkey's biggest regional development plan. In the year 2003, the expenditures exceeded 16.6 billion US dollars (T.C. Başbakanlık).

The water resource plan of the project includes construction of 22 dams, 19 hydroelectric power plants and irrigation of 1.82 million hectares of land. The proposed components of GAP master plan has four main objectives which are developing and managing soil and water resources for irrigation, industrial and urban uses in an efficient manner; improving land use through optimal cropping patterns and agricultural practices; promoting agro-industry and those based on indigenous resources and providing better social services, education and employment opportunities to control migration and to attract qualified personnel to the area (Ünver, 1997). Irrigation assistance services including on-farm development works and efficient use of water are among the most important components in the establishment of an efficient irrigation system in the region (Akuzum et. al., 1993)

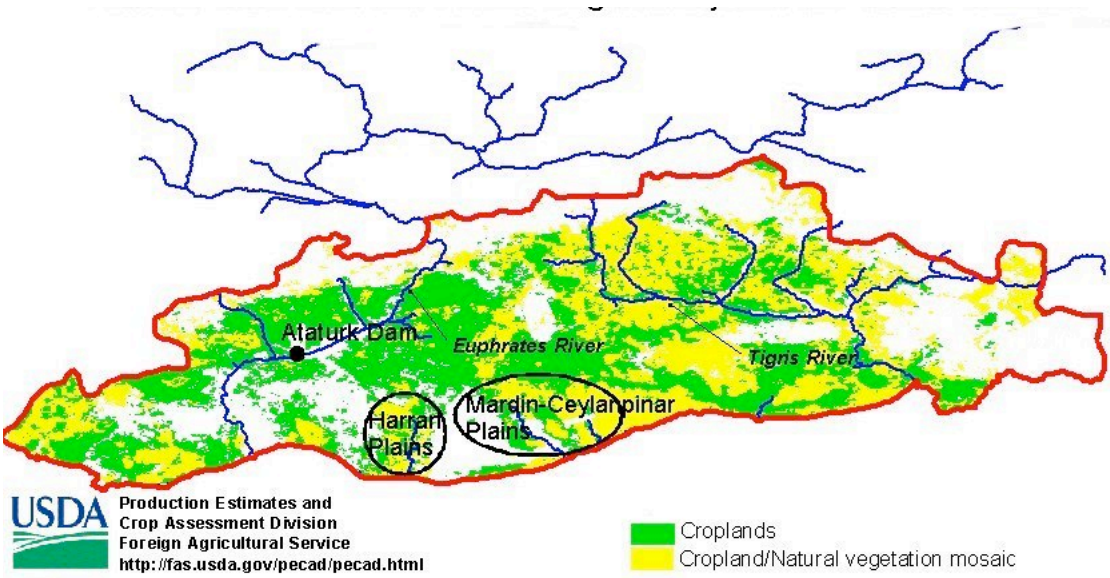

Figure1.4 Atatürk Dam and the Plains Irrigated by the Şanlıurfa Tunnels (USDA-FAS, 2007)

There are some important facts from the results of the agricultural changes by GAP. As Ünver (1997) estimated, the ratio of irrigated land to total GAP area will increase from 2.9% to 22.8% while that rain-fed agriculture will decrease from 34.3% o 10.7%. Figure.1.4 shows the irrigation processes in the region.

Before the irrigation activities, general dry cropping included mainly wheat, barley, lentils, and pistachios. Cropping intensity will change from 89% to 134%. The most remarkable change will be in cotton cultivation, which will increase from 2.8% to 25%. Together with other 3 important regions for cotton cultivation, southeast Anatolia region will be one of the main cotton centers in Turkey (Figures 1.5 and 1.6).

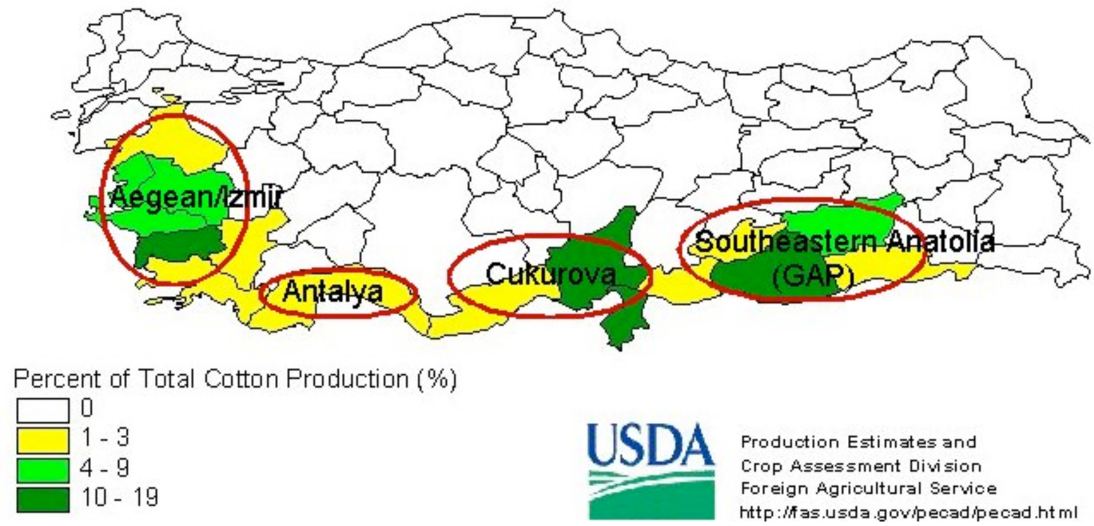

Figure.1.5 Four major cotton regions in Turkey (USDA-FAS, 2007)

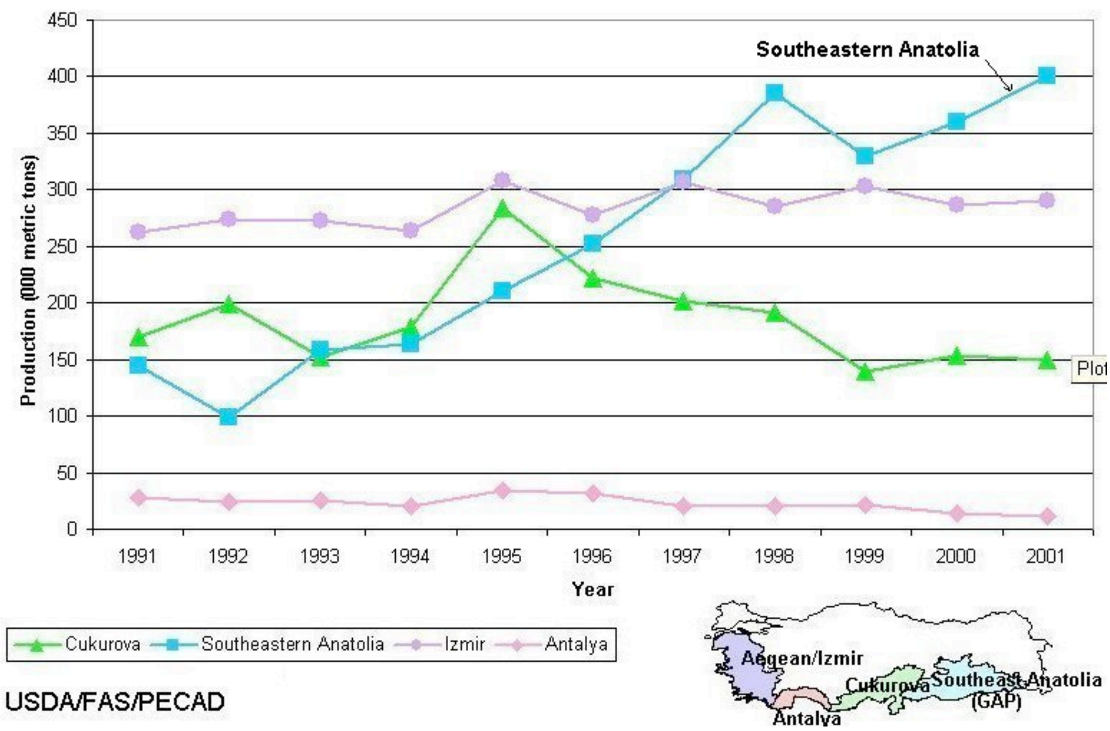

Figure.1.6 Turkey's cotton production by region (USDA-FAS, 2007)

1.3. Previous research

Apart from social and economical studies, there are not so many researches done about the landscape change and irrigation induced climate changes over southeast Anatolia region.

On the climate aspect of previous researches, Komuscu et al. (1998) studied possible climate change impacts on soil moisture availability in Southeastern Anatolia Project region and pointed out that southern and southeastern parts of the region will suffer from severe moisture shortages during summer and added that winter surplus will decrease in scenarios with increased temperature and decreased precipitation in most cases. In addition to this study, Önol (2001) used limited area models to simulate climate effects of a land cover change scenario over GAP region. He indicated that according to the simulation results there was a 20% increase in spring and autumn precipitation values over extremely changed land surface in this region.

Other than climate studies, there are many studies on efficient water usage in semi-arid conditions and crop yield optimization techniques over cultivated areas in Turkey. In their study about non-linear farm optimization under limited water conditions Benli et al. (2003) indicated that the predominant soil type in the GAP area is clay–loam that holds about 150 mm of available water per meter of soil depth. The basic infiltration rate is 13 mm/h. They concluded that the Non Linear Programming model can give higher farm income values then the Linear Programming model under deficit irrigation conditions over this region. Also the relationships between yield and water use for cotton and corn has been reported to be linear (Yazar et al., 2002a); as well as curvilinear (Cetin et al., 2002 and Yazar et al., 2002b) in GAP region.

About the irrigation scheduling techniques and water management in southeast Anatolia, it is shown that the cotton yield is dependant on the production and retention of bolls, and both can be decreased by water stress (Yazar et al., 2002b). In addition to this, Cetin et al. (1994) compared different irrigation methods for effective water use on cotton in the GAP area. They indicated that the highest seed cotton yield was obtained from drip-irrigated plots with 4650 kg ha^{-1} followed by furrow method with 3120 kg ha^{-1}.

As supporting these studies Dağdelen et al. (2006) experimented over cotton and corn cultivation in Aegean region of Turkey and found that S-70 and T- 70 treatments (irrigation applied at the rate of 70%) could be used as a good basis for reduced irrigation strategy development in semi-arid regions where irrigation water supplies are limited.

About land surface modeling and land surface atmosphere exchanges, there is a big consensus around the world. Most of the studies in the literature agree that land surface is closely related to the overlying atmosphere and affects main energy transfer processes to the atmospheric general circulations. As one of the important studies, Adegoke et al. (2007) experimented over central U.S. and simulated land cover change impacts on climate conditions. They concluded that simulation results for a model domain centered over Nebraska indicate significant differences in the surface energy fluxes between the irrigated (control) and non-irrigated (dry) simulations. Surface latent heat flux was higher by 36% and dew point temperature was higher by 2.3 to 8 ^{o}C in the control simulation. Also, surface sensible heat flux of the control simulation was 15% less and the near-ground (2 m) temperature was 1.2 to 8 ^{o}C lower compared to the dry run, indicating irrigation-induced surface cooling effect.

For the Canadian part of North America, Raddatz (2007) also found evidence for land use impact on weather and climate. In his study, he stated that the physiological and physical properties of the vegetation, along with the land cover’s impact upon the level of available soil moisture, affect the weather and climate by influencing the transfer of heat, moisture and momentum from the land surface to the overlying air.

For southeast Asia, Sarkar et al. (2007) also found similar results for impact of land cover change on climate. Their study over cultivated areas of southeast China showed that agrarian activities exert maximum influence on summer rainfall due to spring time irrigation of these areas altering the surface and radiation budget and Bowen’s ratio.

Lastly there is also evidence that anthropogenic land cover change has an estimated effect on the arid lands of central Asia. Lioubimtseva et al. (2005) have pointed out over central Asia plains that local and regional human impacts in arid zones can significantly modify the surface albedo, as well as water exchange and nutrient cycles that could have impacts on the climatic system both at the regional and global scales.

1.4. Scope of the work

This work is intended to cover recent climate change issues over southeastern Turkey. After giving a brief introduction of GAP and southeast Anatolia region, the investigation of possible climate differences are described here. From the experiment design through materials and softwares, the study is explained here concluding with the major findings of the work and concurrent discussions.

1.5. General structure of the paper

To provide a better understanding, this paper is divided into four chapters. After finishing the first introductory chapter here, the second chapter gives deeper information about the experiment design, methods used and the instrumentation. Some theoretical knowledge about the observational tools and the software are also provided in this chapter.

Continuing with the experimental results, the third chapter contains all the analysis phase, findings and visualized data about the work.

Lastly the fourth chapter gives the main discussion issues of the results taken by the experiment and also provides a brief summary with a short conclusion part.

2. METHOD, EXPERIMENT SITE, INSTRUMENTS and MODEL

2.1. Plan

This work is intended to help us realize possible climatic changes over southeastern Turkey during the GAP period. In order to get a scientific idea, analysis of one year long meteorological observations and land-surface model simulations are examined.

To observe and investigate the suspected differences, two locations are chosen for the experiment. One site is chosen to represent the pre-GAP conditions as the control case and the other to represent the direct influence of irrigation from GAP.

Automatic weather stations and eddy-covariance systems are used as the observational instrumentation. The automatic weather stations are operated to gather some general meteorological data like precipitation, insolation, net radiation, temperature, relative humidity, wind speed and wind direction. On the other hand eddy-covariance systems are used to measure and calculate sensible and latent heat fluxes, CO_2 concentrations, average H_2O concentration and carbon flux.

Since the project GAP affected southeastern Turkey over massive scales of land, experiment sites are chosen over the most affected areas like Harran Plain. Northwest part of Harran Plain, near the city of Şanlıurfa, there are several villages and the Osmanbey campus of the Harran University. Osmanbey Campus of the university is located on the boundary of irrigated areas of Harran Plain and shows the land before irrigation has started. This site is chosen as the control case area and one set of the observational equipments was installed here. The second site was chosen in the Çekçek Village that lies in the northern part of this plain. There is an extensive cotton farming activity here by using irrigation from GAP.

After one year long observations, the gathered data could be analyzed and the different outcomes of the two experiment sites could be used to comment on the so called climate change over this region. By doing this, a land surface model simulation could help to examine energy exchanges between atmosphere and land more deeply, so NCAR’s (National Center for Atmospheric Research) CLM (Community Land Model) v.3.0 was used to simulate the abovementioned processes.

With all these described techniques and methods, the answer to the question could be put forward clearly in a scientific fashion.

2.2. Experiment site

As mentioned in the previous section, two sites are chosen for the experiment over the region: Osmanbey Campus of Harran University in Şanlıurfa and Çekçek Village in the northern Harran Plain.

2.2.1. Osmanbey

The Osmanbey Campus of Harran University lies in 18 km east of Şanlıurfa (37.10 N 38.59 E). This campus is located on an arid site where there is no farming activity and very rare vegetation nature is present all year. The general surface characteristics of this region represent the surrounding areas before irrigation activities have started. This is a proper experiment site to observe the pre-GAP conditions. The observational tools are installed near the Osmanbey Campus Arboretum.

2.2.2. Çekçek

Çekçek Village is 13 km east of Şanlıurfa (37.08 N, 38.56 E). The village lies in the green fields of northern Harran Plain. Although there is corn and wheat farming together with cotton all around the Harran Plain, there is only cotton farming activity in Çekçek area. The observational tools are installed in a cotton field among the crops. Due to the cotton farming activities, there is very rare vegetation during the winter, but starting from May, crops dominate the region and all the area is covered with green cotton plants during summer until early September. By gathering data from this site, the analysis will show direct influence of irrigated farming over the climatic parameters.

2.3. Observational equipments

As described before, automatic weather stations, eddy covariance systems and a land surface model (CLM) are the tools used in this experiments.

2.3.1. Automatic Weather Stations

For the observations of several meteorological parameters, two automatic weather stations are installed in the experiment sites. These stations include sensors for net radiation, temperature, relative humidity, wind speed, wind direction and rain gauges to measure precipitation. There are solar panels attached to each weather station. The energy requirements are supplied from mains as well as solar energy by these panels. Also two data loggers stored the gathered data from the stations. Rotonic MP101 air temperature and relative humidity sensors are located nearly 2 meters above the ground. RM Young 03001 wind speed and direction sensors are embedded to the system at 2.5 meters altitude. CM 6B pyranometer is attached to the system with a height of 2 meters above ground. LSI DQA rain gauges are positioned near to the main weather stations. 10 W solar panels are attached to the system with a proper angle. The stations also include SC32 A RS232 interfaces, CR10X data logger and a tripod kit.

2.3.2. Eddy-covariance systems

Energy exchange processes and some chemical concentrations are generally observed with eddy covariance systems. To define the surface atmosphere interactions, its essential to examine these mechanisms. Thus two eddy covariance systems are located in the experimental sites. These tools have observed sensible and latent heat fluxes, CO_2 and H_2O concentrations and carbon flux.

These systems include CR5000 data loggers, CSAT3 3D sonic anemometers and CS7500 LiCor Open Path CO_2 /H_2O Analyzers.

2.4. Modeling

2.4.1. Land surface models and CLM

Land surface models are essential parts of all Global Circulation Models (GCM)/Limited Area Models (LAM) or any other atmospheric model. Nowadays there are several land surface models being used all around the world. Every GCM or LAM uses a different type of land surface model. Thus certain differences occur in simulations of land surface processes because of different parameterization for surface albedo and vegetation types in the land surface model.

CLM is a modular part of NCAR's CCSM (Community Climate System Model). It is a rather new model comparing to other famous land surface models like BATS, SiB, SiB2, IAP94 and LSM. It is developed by evaluating BATS, IAP94 and LSM in NCAR (Oleson et. al., 2004). The main purposes for this new model were to focus on carbon cycling, hydrology, river routing and ecosystem modeling. Being used as the land surface part of NCAR's CCSM and CAM (Community Atmosphere Model), CLM 3.0 is a single column, multi vegetation type, hydrological model. Dynamic vegetation structure and river transport algorithms are the main important advantages of CLM 3.0. It can be used as coupled to climate system model CCSM or atmosphere model CAM and also as a stand-alone version of offline simulation. In the offline version of CLM, some atmospheric parameters must be given as input to the model and the model reads in these data periodically (Table.2.1).

Table.2.1 Input parameters to CLM 3.0 offline version

[1]Reference height	z_{atm}	m
Zonal wind at z_{atm}	u_{atm}	m s^{-1}
Meridional wind at z_{atm}	v_{atm}	m s^{-1}
Potential temperature	$\overline{\theta_{atm}}$	K
Specific humidity at z_{atm}	q_{atm}	kg kg^{-1}
Pressure at z_{atm}	P_{atm}	Pa
Temperature at z_{atm}	T_{atm}	K
Incident longwave radiation	$L_{atm}\downarrow$	W m^{-2}
[2]Liquid precipitation	q_{rain}	mm s^{-1}
[2]Solid precipitation	q_{sno}	mm s^{-1}
Incident direct beam visible solar radiation	$S_{atm}\downarrow^{\mu}_{vis}$	W m^{-2}
Incident direct beam near-infrared solar radiation	$S_{atm}\downarrow^{\mu}_{nir}$	W m^{-2}
Incident diffuse visible solar radiation	$S_{atm}\downarrow_{vis}$	W m^{-2}
Incident diffuse near-infrared solar radiation	$S_{atm}\downarrow_{nir}$	W m^{-2}

The CLM 3.0 provides heat fluxes, surface and vegetation albedos, meridional and zonal surface stresses as output. These parameters can easily be used as input to other atmospheric models, or as control values like in this paper.

2.4.2. CLM structure

The data structure of CLM 3.0 is mainly subgridded into hierarchical levels. For the computing time efficiency and memory allocations, these levels work separately and some parameters are added up to a higher level when necessary. The different sub grid categories are shown in the Figure.2.1. This data structure is the backbone of the main iteration algorithm. This nested sub grids can contain multiple land units, columns and plant functional types (Oleson et. al. 2004).

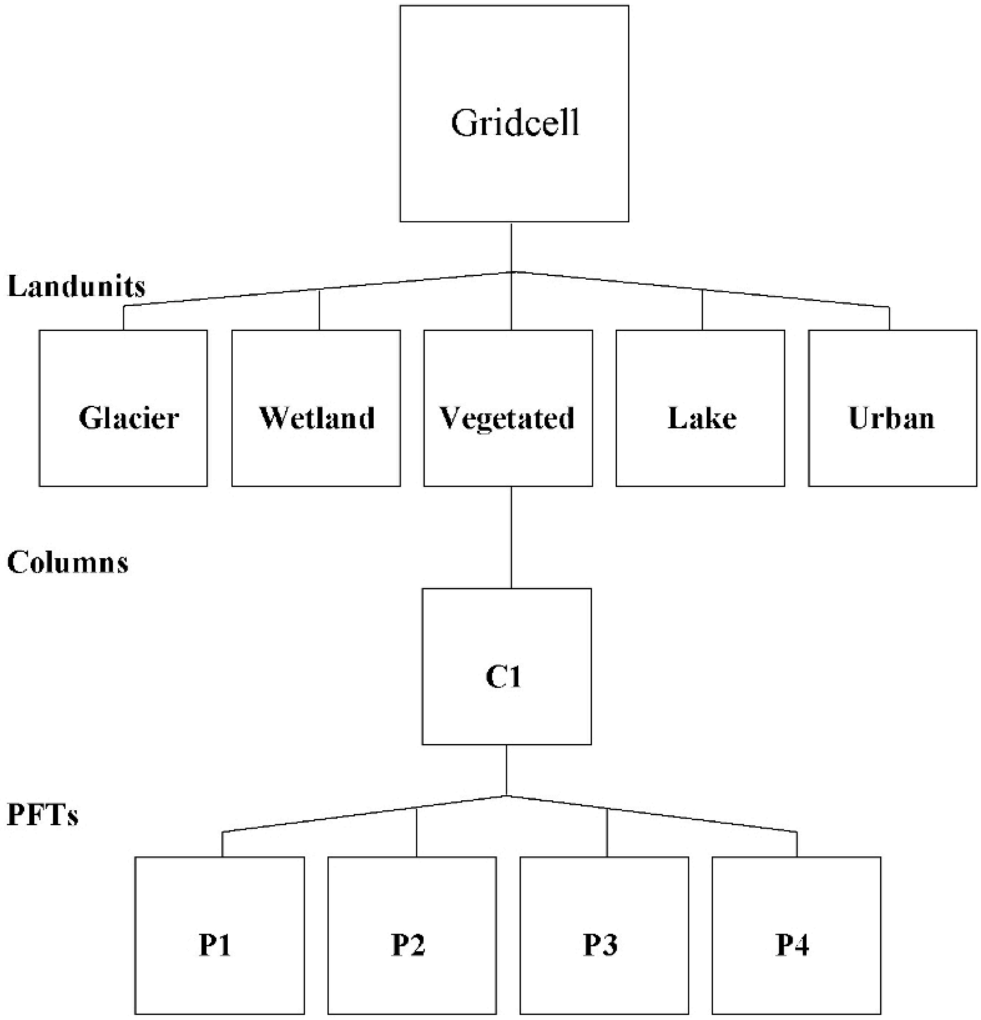

Figure.2.1 Subgrid hierarchy in CLM

In every simulation the experimental areas can contain many grid cells. Each grid cell can include different number of land units, these land units can be subgridded into several columns and each column can contain up to 4 pfts (plant functional type) of 15 pfts.

As shown in the figure above different types of land units include glaciers, wetlands, vegetated areas, lakes and urban settlements. These land units are meant to capture physical soil properties of different land covers. So the soil textures, colors and other soil related parameters are initialized in this level.

Under each land unit, columns are regulating the soil and snow states. Water and energy state variables are adjusted here. Some of the parameters in these columns are weighted averages of corresponding pfts under that column.

The last sub grids, pfts, are mainly responsible for capturing the biogeophysical and biogeochemical differences of multiple vegetation types. There are 15 different pfts (Table.2.2) and each column can be composed of up to 4 of these pfts.

Table.2.2 PFTs available in CLM 3.0

Plant functional type	Acronym
Needleleaf evergreen tree – temperate	NET Temperate
Needleleaf evergreen tree - boreal	NET Boreal
Needleleaf deciduous tree – boreal	NDT Boreal
Broadleaf evergreen tree – tropical	BET Tropical
Broadleaf evergreen tree – temperate	BET Temperate
Broadleaf deciduous tree – tropical	BDT Tropical
Broadleaf deciduous tree – temperate	BDT Temperate
Broadleaf deciduous tree – boreal	BDT Boreal
Broadleaf evergreen shrub - temperate	BES Temperate
Broadleaf deciduous shrub – temperate	BDS Temperate
Broadleaf deciduous shrub – boreal	BDS Boreal
C_3 arctic grass	-
C_3 grass	-
C_4 grass	-
Crop1	-
[1]Crop2	-

These PFTs differ in physiological and morphological traits along with climatic preferences (Bonan et. al. 2002b). As with the primary vegetation types like broadleaf, needle leaf deciduous, evergreen trees, shrubs, crops and grass, there is also bare ground option in the model. Each pft differ in aerodynamic parameters, optical properties, root distributions and photosynthetic parameters. These parameters are taken from previous studies. Root distributions are taken from Zeng (2001) and other parameters from Bonan et. al. (2002a). The default mode of operation in CLM requires all available pfts in a single soil column competing for water (Vertenstein et. al., 2004).

CLM 3.0 works in a combined algorithm fashion. There are four main processes calculated by the model. These are biogeophysics, hydrological cycle, biogeochemistry and dynamic vegetation (Oleson et. al., 2004).

Biogeophysics

At this part of the model, the instantaneous exchanges of energy, water, and momentum with the atmosphere are handled. The main concepts in this part concern aspects of micrometeorology, canopy physiology, soil physics, radiative transfer, and hydrology. As seen in the Figure.2.2 below, these processes are connected to each other through a complex system of feedbacks from different parts of the environment.

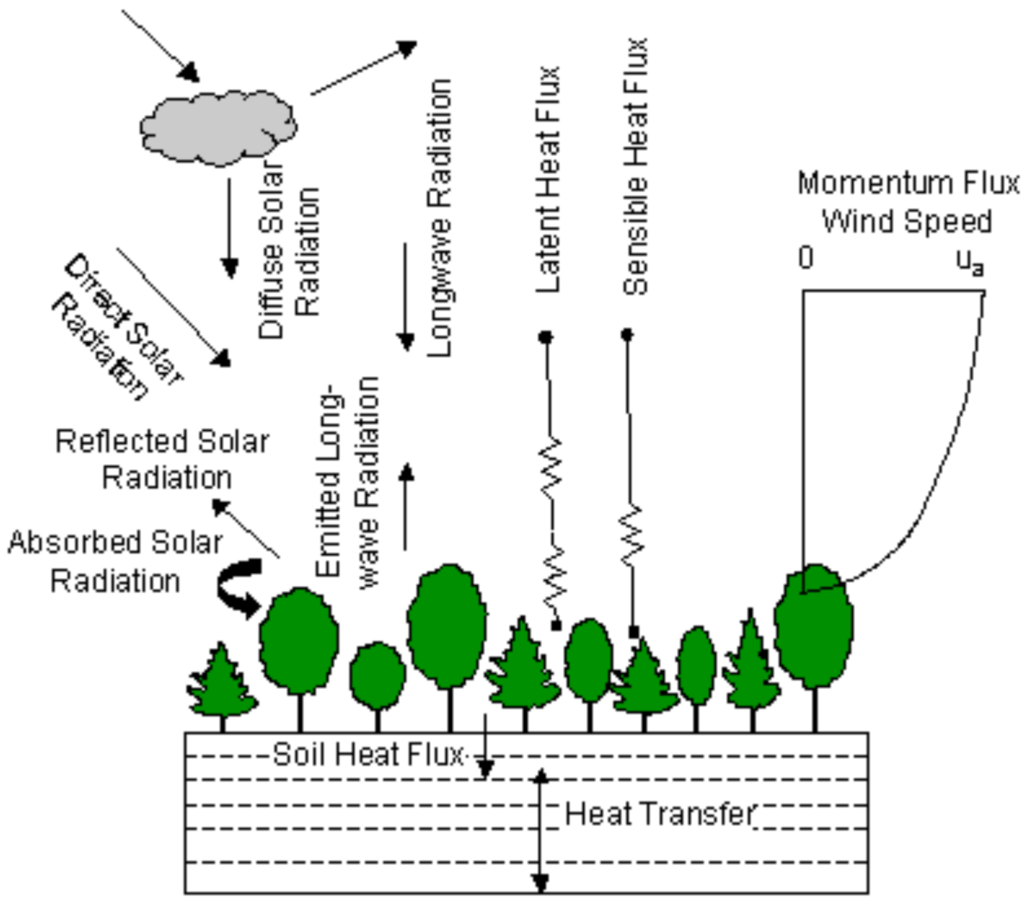

Figure 2.2 Biogeophysics of CLM (Bonan, 2002b)

Hydrological cycle

The hydrologic cycle over land includes interception of water by plant foliage and wood, through fall and stem flow, infiltration, runoff, soil water, and snow. These are directly linked to the biogeophysics and also affect temperature, precipitation, and runoff (Figure.2.3).

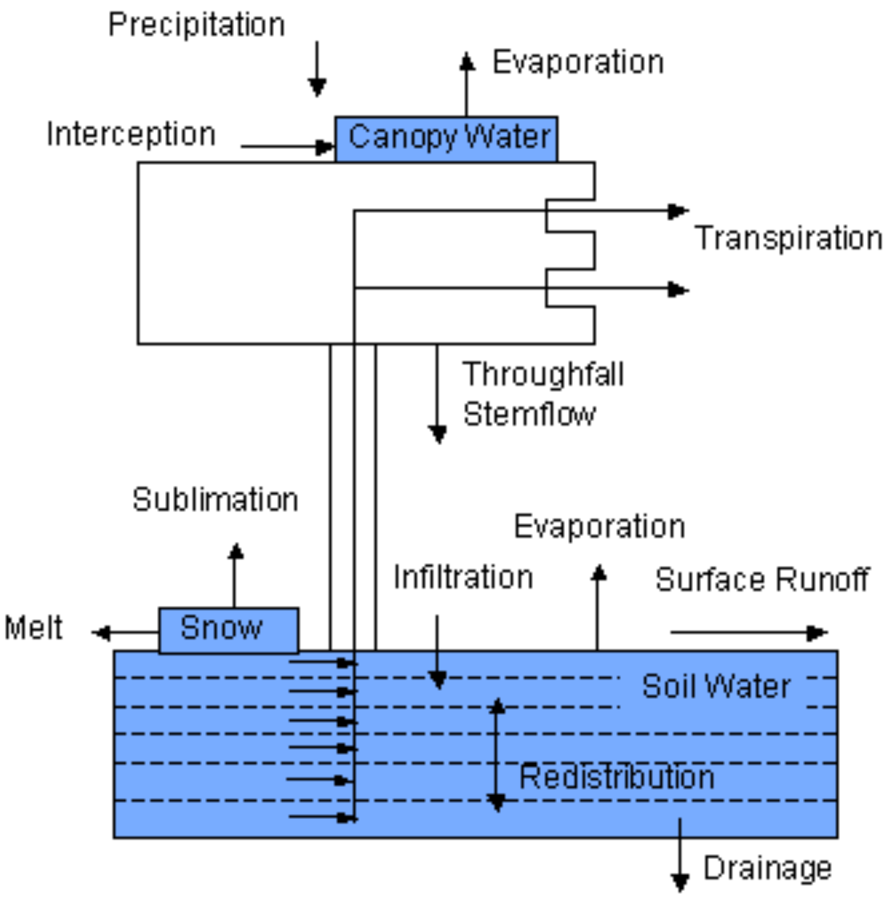

Figure.2.3 Hydrology of CLM (Bonan, 2002b)

There is also a river routing process in CLM. Total runoff (surface and sub-surface drainage) is routed downstream to oceans using a river routing model (Figure.2.4).

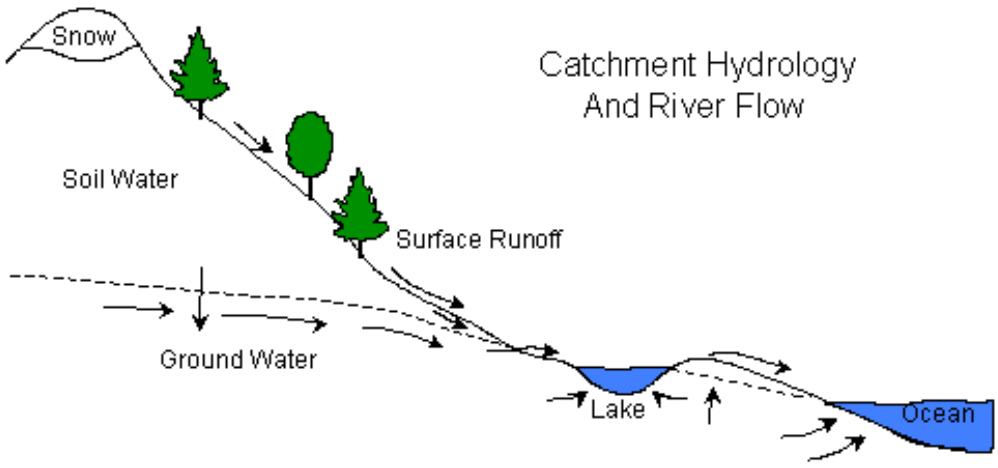

Figure.2.4 River Routing Model of CLM (Bonan, 2002b)

Major global river systems are clearly evident in the model output (Figure.2.5).

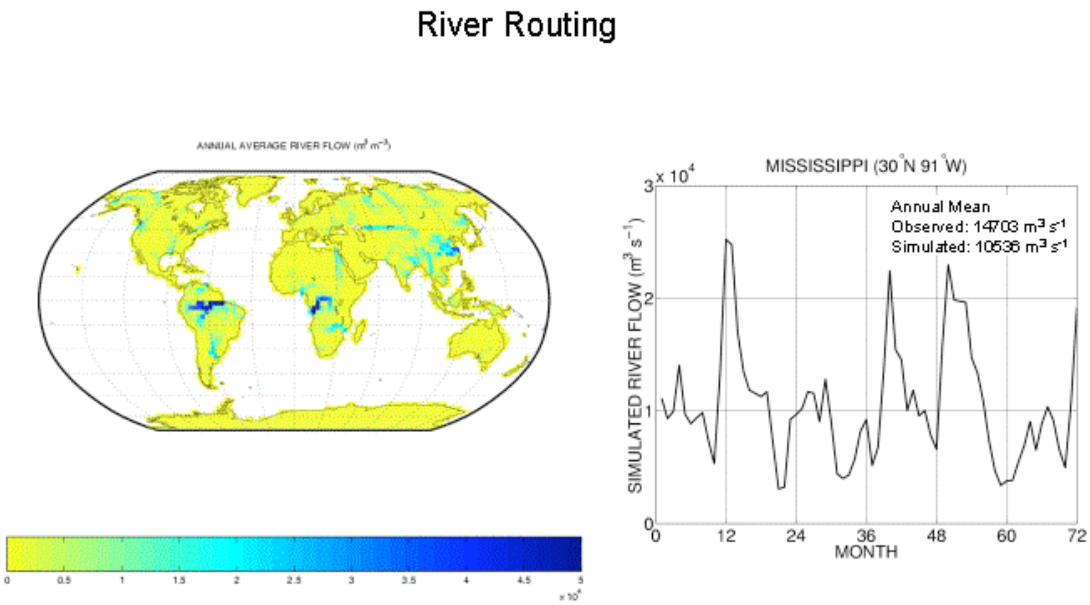

Figure.2.5 River systems in CLM River Routing Model (Bonan, 2002b)

Biogeochemistry

This is the instantaneous exchanges of chemical constituents with the atmosphere. Current projects include: carbon, biogenic volatile organic compounds, dust, dry deposition (Figure.2.6).

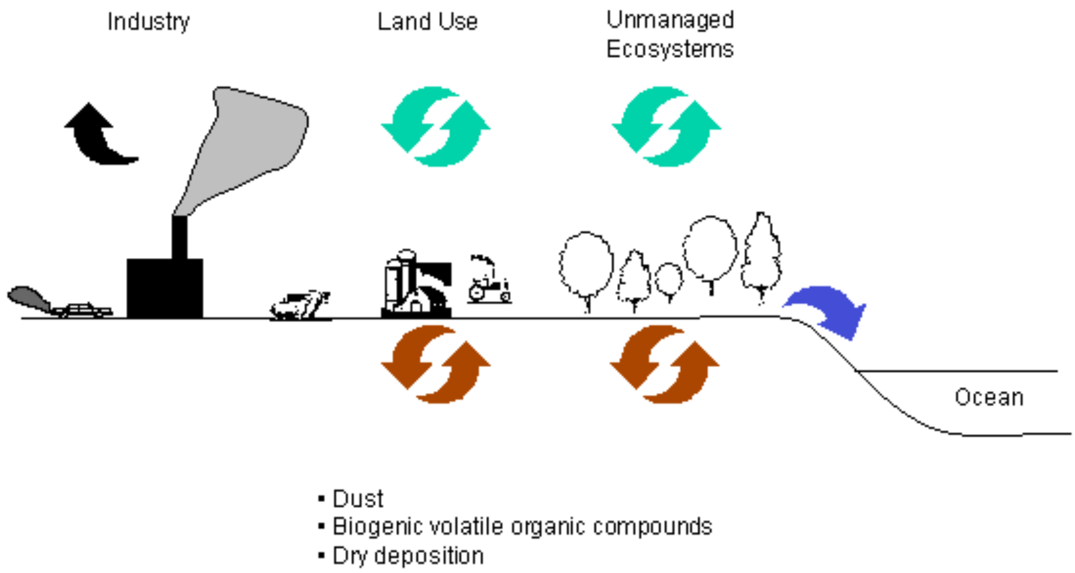

Figure.2.6 Biogeochemistry of CLM (Bonan, 2002b)

Dynamic vegetation

Ecosystem carbon balance includes the carbon cycle but also changes in community composition and vegetation structure in response to disturbance (e.g., fire, land use) and climate change (see Figure.2.7).

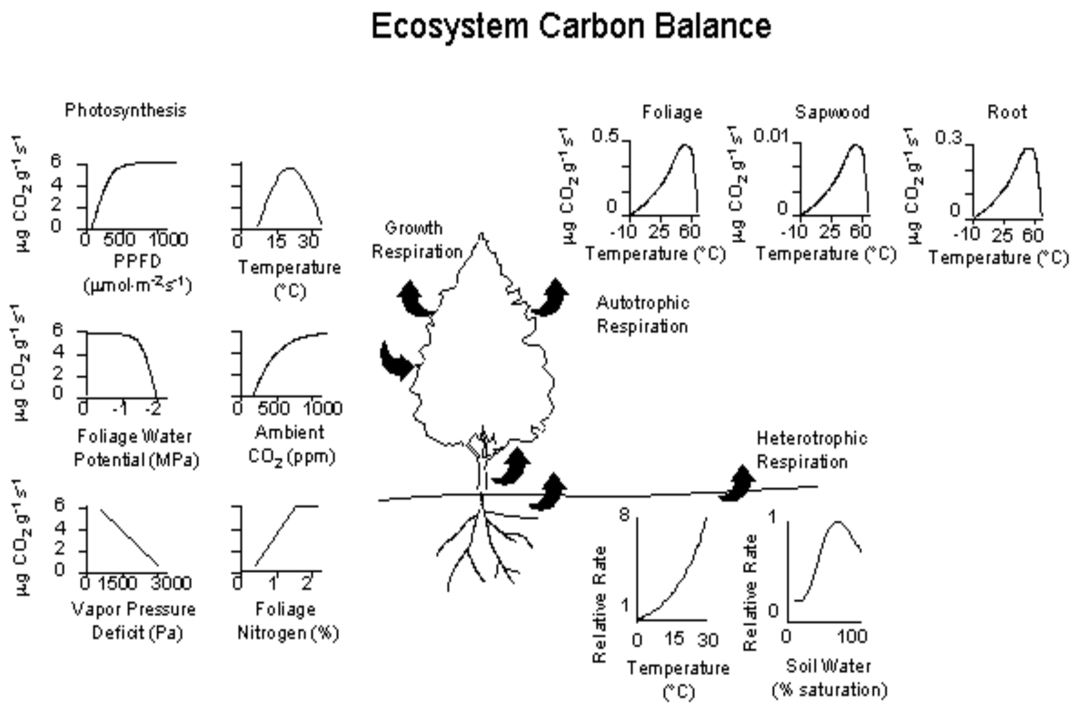

Figure.2.7 Ecosystem carbon balance of CLM (Bonan, 2002b)

There are two time-scales for the Succession and Biogeography part dynamics: Succession considers changes in community composition and vegetation structure over periods up to several hundred years, typically following disturbance such as fire or land use. Over longer-periods of times (e.g., centuries, millennia) the biogeography of vegetation changes in response to climate change (Figure.2.8).

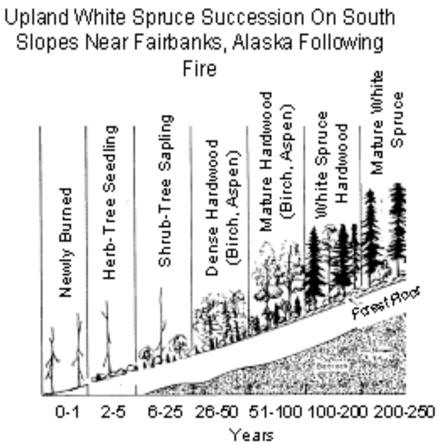

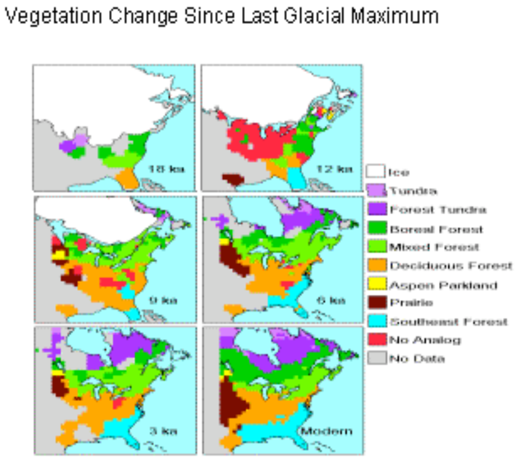

Figure.2.8 Vegetation change in CLM (Bonan, 2002b)

There are two main projects related to dynamic vegetation. Peter Thornton from NCAR is leading an effort to add the carbon and nitrogen cycles to the Community Land Model. This uses carbon and nitrogen parameterizations of the BIOME-BGC model. Vegetation structure (e.g., leaf area index, carbon pools) changes over time, but community composition is prescribed. Gordon Bonan and Sam Levis of NCAR are leading an effort to allow for dynamic community composition. The current implementation of dynamic vegetation uses many of ideas formulated in the Lund-Potsdam-Jena dynamic global vegetation model.

This single column biogeophysical land surface model, CLM, can be run serially on a laptop computer as well as in parallel with distributed or shared memory processors (Hoffman et. al., 2004). In this experiment, offline version of the model is used on a serial working platform.

2.4.3. Calibrations

Before initializing the model simulation, some physical and physiological parameters should be adjusted. These adjustments are succeeded by calibrating the model to the studied experiment site.

Vegetation type choosing:

In CLM, as described in the previous sections, the land is divided into several sub grids and plant functional types. In order to represent the experiment site correctly some adjustments are performed. Since Osmanbey area is mostly bare ground, there was no big problem there. But with Çekçek area the partitioning of cotton plants and noncultivated areas was needed to be adjusted.

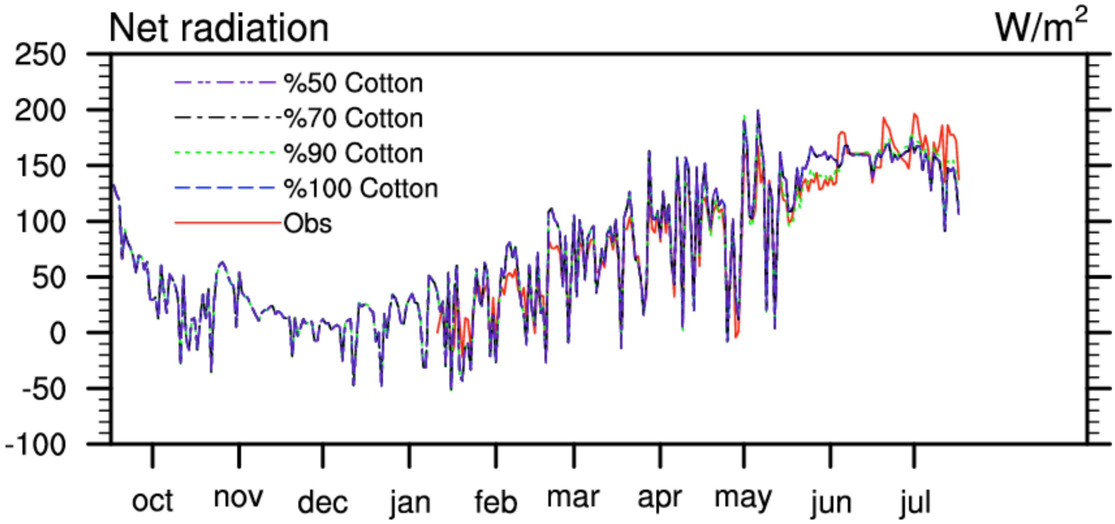

Figure.2.9 Calibration plot of vegetation type (all year)

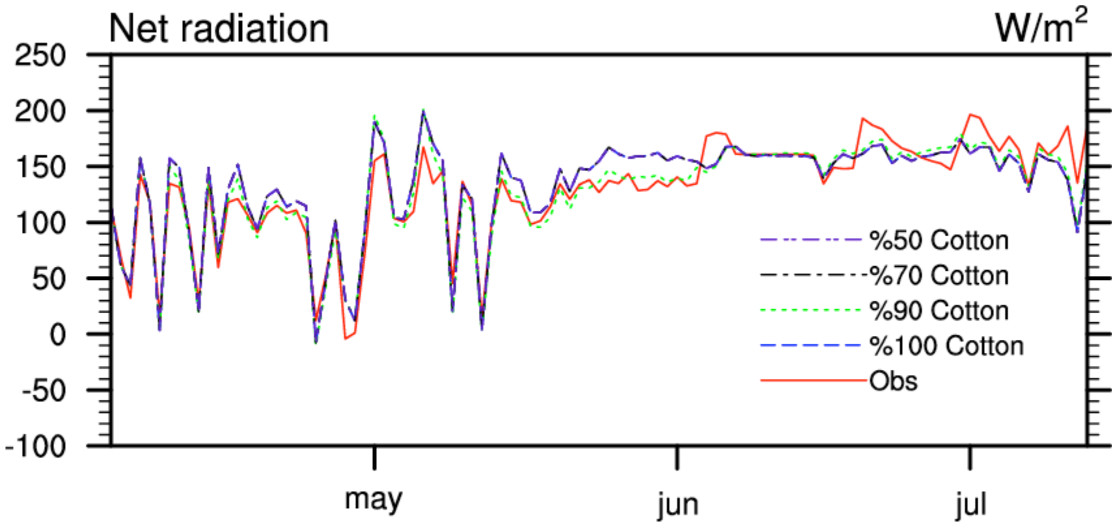

Figure.2.10 Calibration plot of vegetation type (May-June-July)

As it is seen from the plots (Figure2.9 and Figure 2.10), by evaluating the observed net radiation versus several vegetation type tests, 10% bare ground / 90% cotton gives the best results for Çekçek site.

Soil color choosing:

After resolving the correct vegetation type, soil color parameter was needed to be calibrated. Again, since Osmanbey area is bare ground and the default soil color value from CLM (soil color = 3) was enough to represent the area, no calibration was needed for it. Contrarily, in Çekçek different soil colors were tested and the results are shown in the figures below (Figure.2.11 and Figure.2.12).

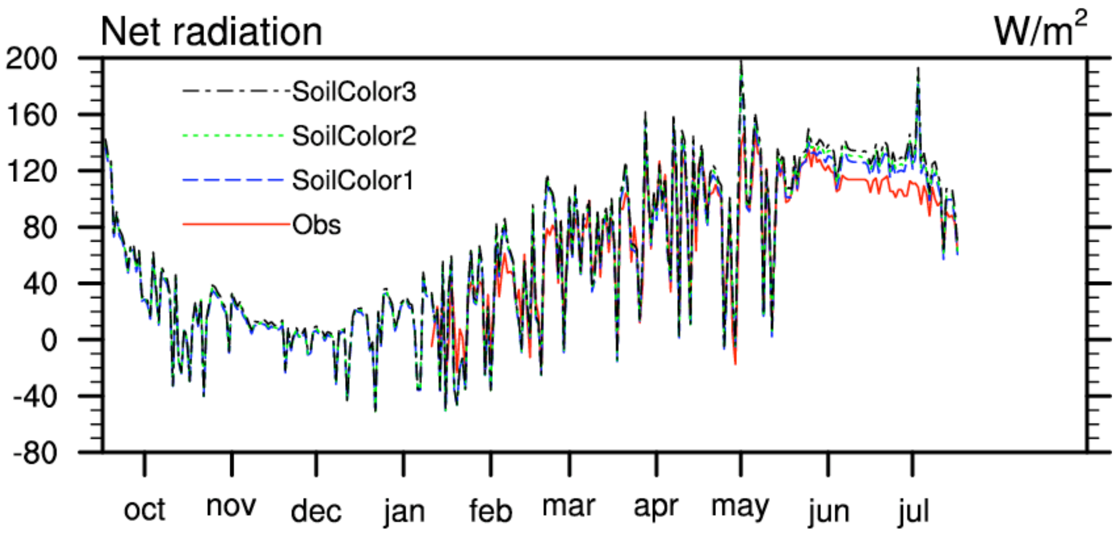

Figure.2.11 Calibration plot of soil color (all year)

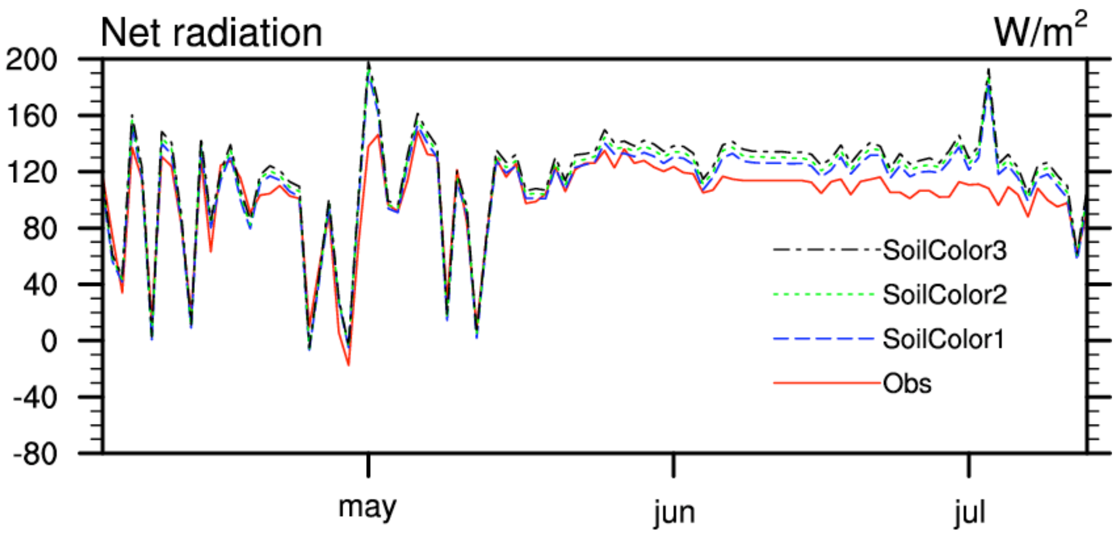

Figure.2.12 Calibration plot of soil color (May-June-July)

As it is clearly significant from the plots, soil color 1 is the most realistic choice. In CLM soil color with soil moisture defines the albedo and higher soil color gives lower albedo values and hence higher net radiation. So in this simulation soil color 1 provided larger albedo values.

3. ANALYSIS and RESULTS

3.1. Analysis

The data used in this work consist of the observations gathered from 15 September 2006 to 24 August 2007. The hourly and daily averaged data from the automatic weather stations and 30-min averaged data from eddy covariance systems are used in this study. Stored observational data in the data loggers are regularly downloaded in every two weeks by field trips. It is well known that the theoretical techniques for observational tools never work as expected in nature.

In general the automatic weather stations keep more healthy records of data, while the more complicated eddy covariance systems are more affected from tiny disturbances and sometimes producing faulty, unmeaningful records. Due to their sensitive structure and mechanisms, several things can cause miscalculations to occur. Any physical interference or severe weather conditions like extreme precipitation or wind result in unexpected data production from these systems. Apart from these problems, the systems can stop producing data for weeks after a disturbing interference.

The analyzing phase of the experiment required a noteworthy effort of refining. To prepare a healthy set of data, it was needed to define the missing data parts and filling these gaps with missing flags for visualization. For the model simulation, it was needed to prepare a set of input with full data, in which there is no missing parts. So, for the model input the missing parts of the data was filled by linear interpolations in little gaps, or weekly averaged values of 1 week before and 1 week after of the missing parts and also sometimes it was logical to fill in the missing part of one set of data from the other set like Osmanbey from Çekçek or Çekçek from Osmanbey.

Also the extreme and unmeaningful records that caused by physical contacts and brutal weather conditions was filtered out to obtain only the necessary records. Especially during the times of downloading the records from the data loggers or necessary cleaning of dirty sensors, there is an obvious system malfunction in data productions. These faulty and unnecessary records were cleaned out by scientifically logical filterings.

Completing the healthy sets of data, resulted a meaningful period of 20 September 2006 to 23 August 2007 for visualizations. And for the simulation inputs the set was prepared for the dates from 1 October 2006 to 31 July 2007. Adding to this the net radiation sensors were embedded to the systems in January 2007, so there was no available data for net radiation before this date.

By using these data sets the available parameters are visualized using NCL (NCAR Command Language). Precipitation, insolation, net radiation, temperature, relative humidity, wind speed and wind direction values from the automatic weather stations and carbon flux, CO_2/H_2O concentrations, sensible and latent heat fluxes from the eddy covariance systems are plotted for the study.

3.2. Observational results

Observations from the two sites in upper Harran Plain revealed one year long data for scientific studies. Osmanbey data (pre-GAP) and Çekçek data (post-GAP) are compared in the following figures. From the automatic weather stations there are several meteorological parameters and all of them are visualized and shown in the following pages.

In the figure below (Figure.3.1) daily total precipitation values show a similar pattern over both sites. Most of the precipitation falls in winter months as parallel to the general climate characteristics of the region. There is only a remarkable difference in the end of October and beginning of November, when more rain has fallen over Çekçek area than Osmanbey.

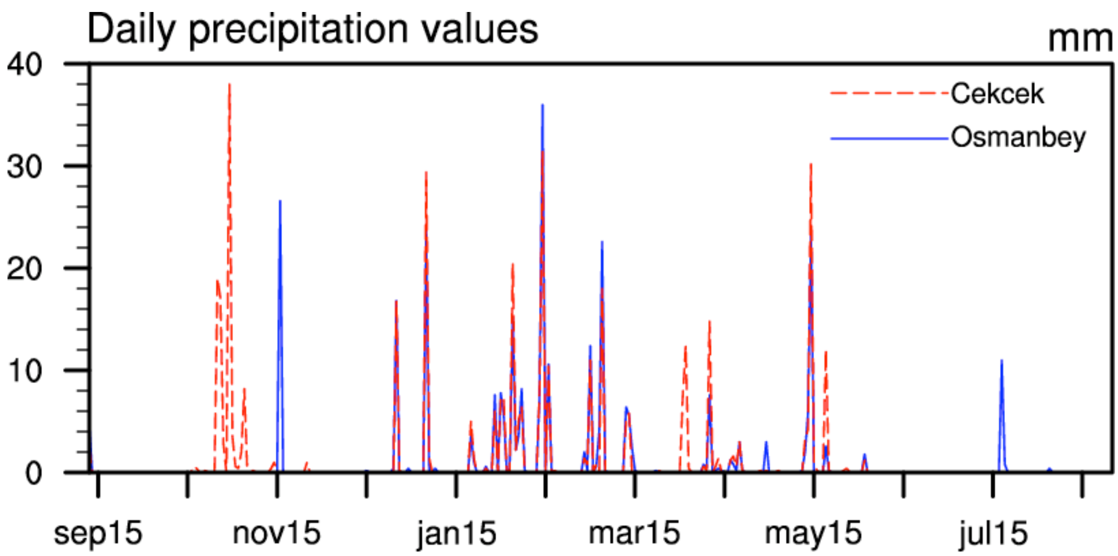

Figure.3.1 Daily precipitation values for Osmanbey and Çekçek

If insolation parameter is observed, it is seen that the one year pattern is shown as expected. Lower values in winter months are increasing through spring where they peak in summer months. Most of the time period, the values go very close to each other in Osmanbey and Çekçek site. But there is a little difference during the last days of the experiment, July and August. During these dates in Çekçek observations, there are relatively lower values of insolation comparing to Osmanbey (Figure.3.2).

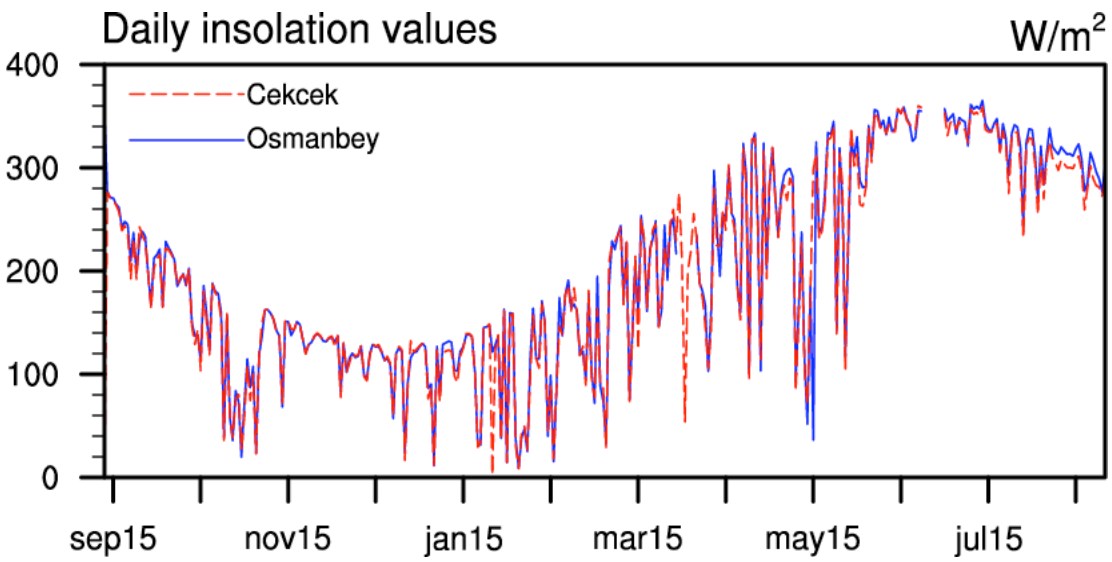

Figure.3.2 Daily averaged insolation values for Osmanbey and Çekçek

If observed closely from February (Figure.3.3) and August (Figure.3.4), it is clear that during the winter values go very close to each other; but there is a difference in summer months (Figure.3.5).

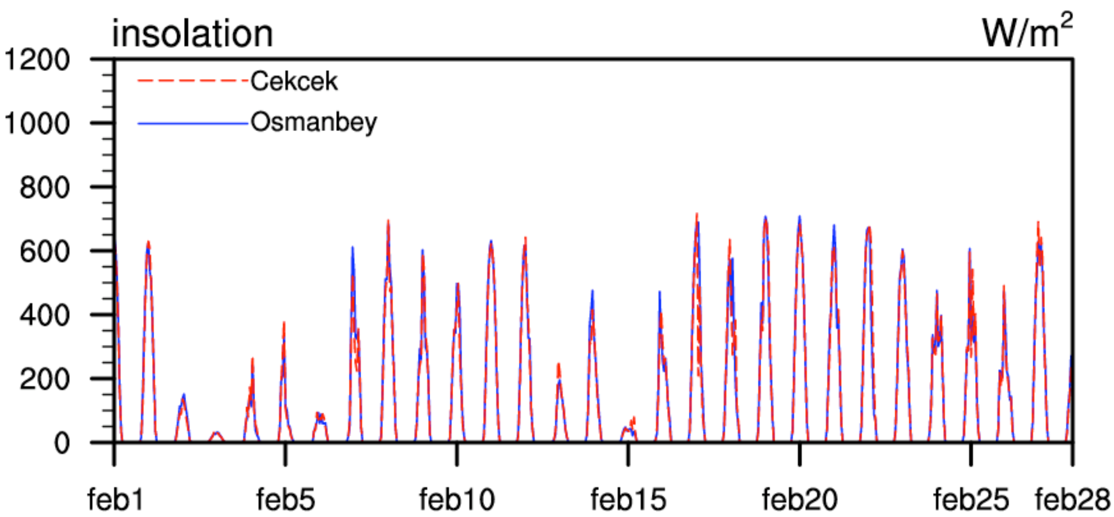

Figure.3.3 Hourly insolation data for Osmanbey and Çekçek (February)

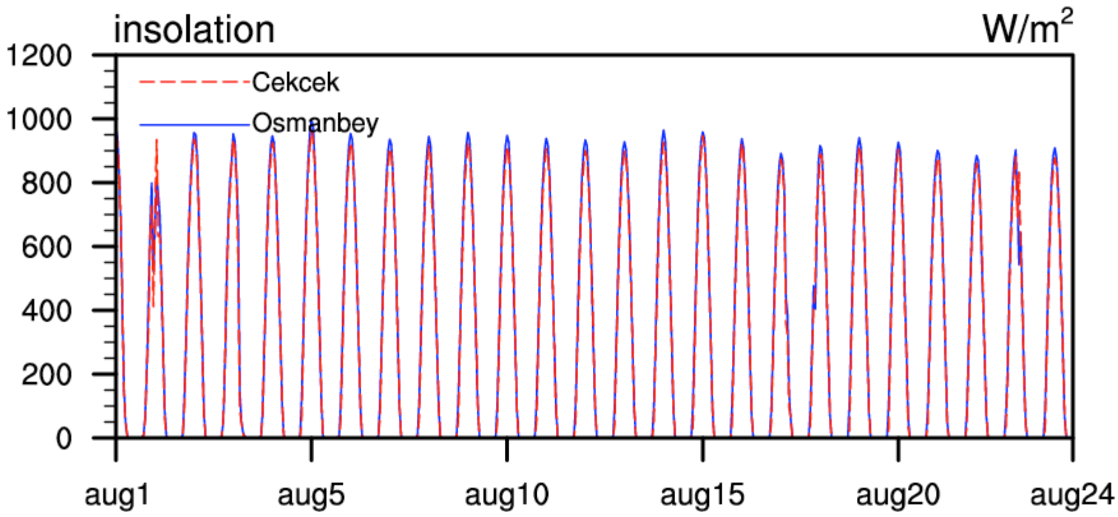

Figure.3.4 Hourly insolation data for Osmanbey and Çekçek (August)

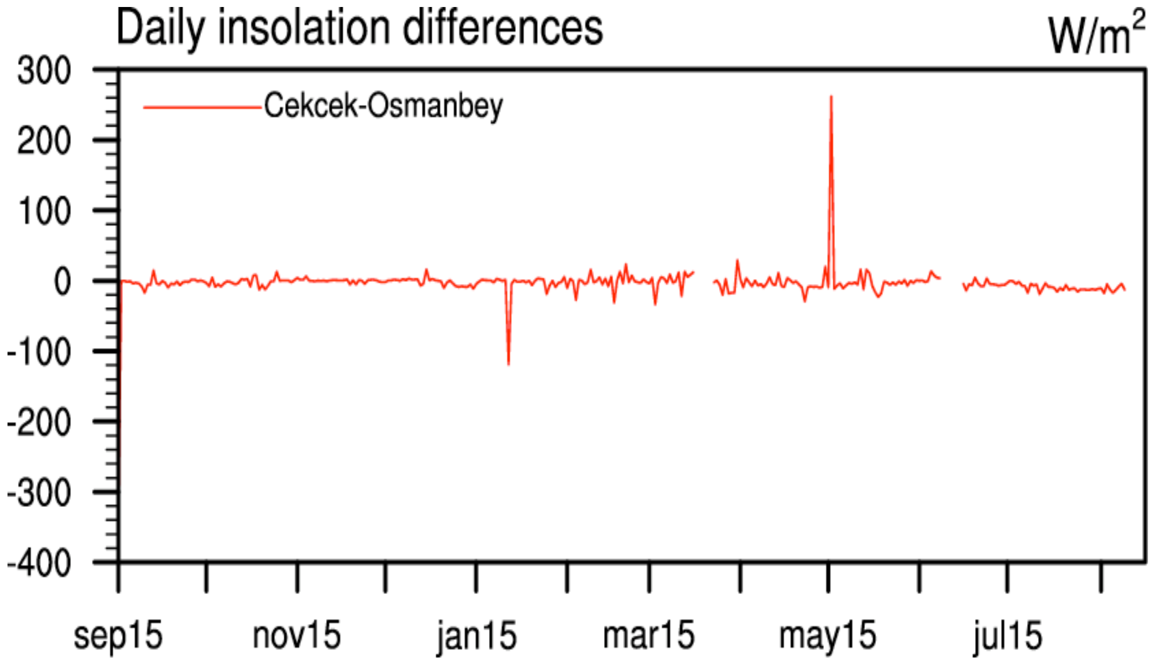

Figure.3.5 Differences in daily insolation values for Osmanbey and Çekçek

It was indicated before that the net radiation sensors are embedded to the systems in January and thus there is data available only after this date. Daily net radiation from both sites takes similar values until June when they start to separate from one another. Starting from the beginning of June, there is more net radiation available on the surface in Çekçek site (see Figure.3.6). In contrast, Osmanbey net radiation values start to decline from June. One can look at the monthly plots (Figure.3.7 and Figure.3.8) and see the difference more closely (Figure.3.9).

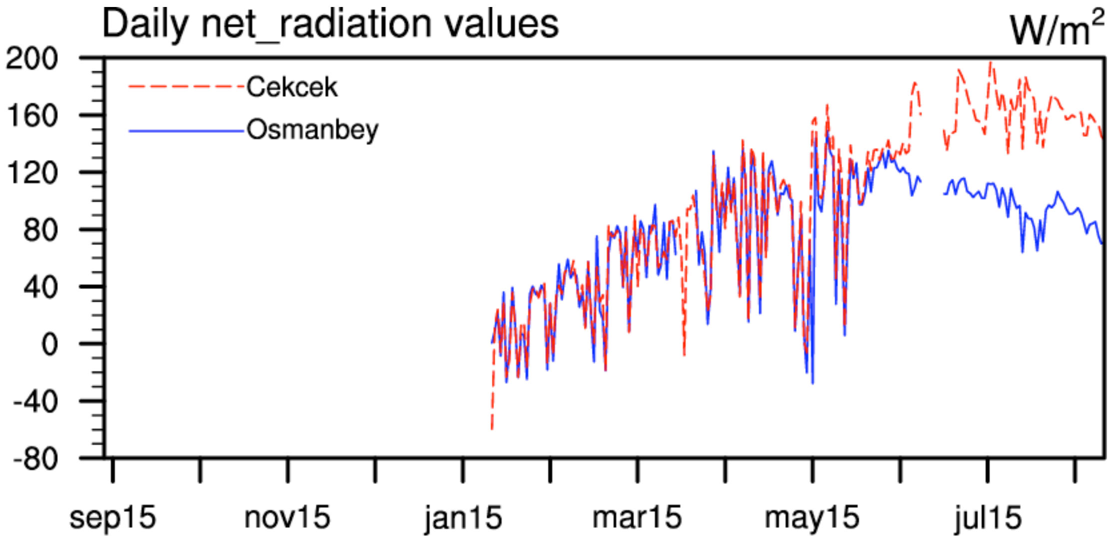

Figure.3.6 Daily averaged net radiation values for Osmanbey and Çekçek

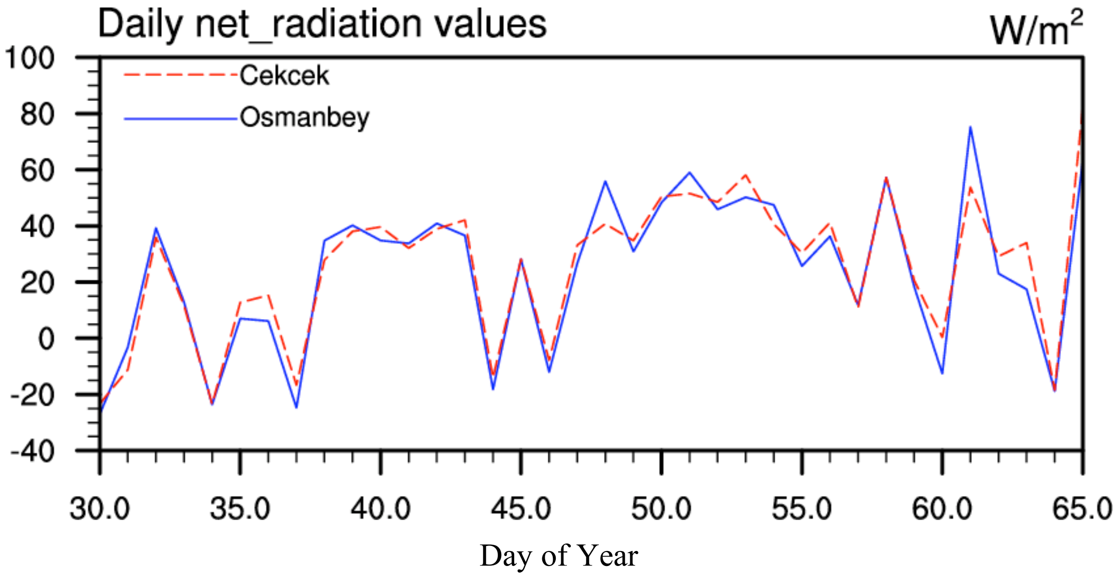

Figure.3.7 Daily averaged net radiation data for Osmanbey and Çekçek (February)

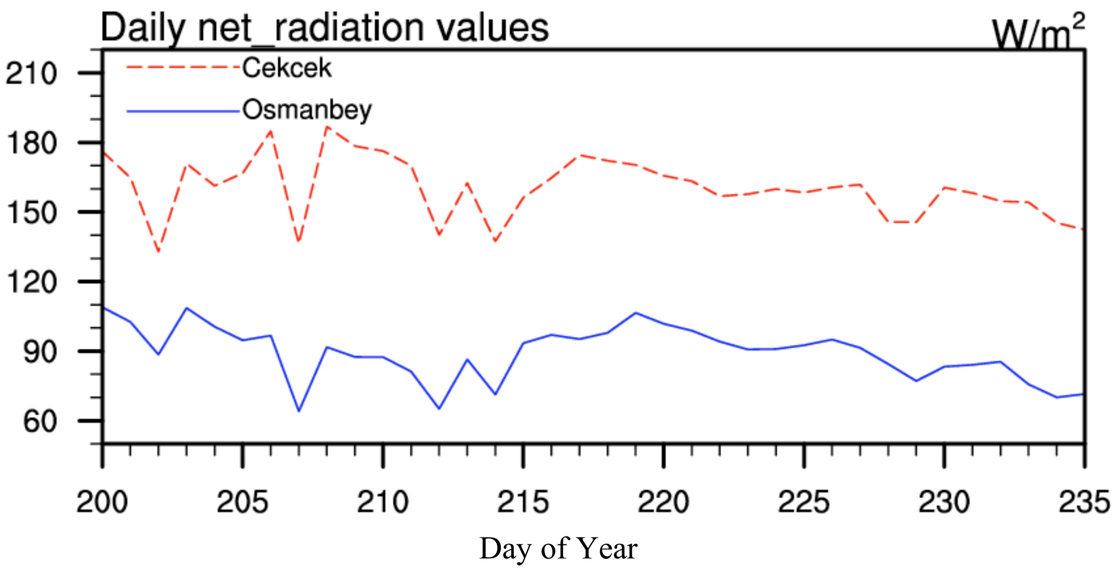

Figure.3.8 Daily averaged net radiation data for Osmanbey and Çekçek (July)

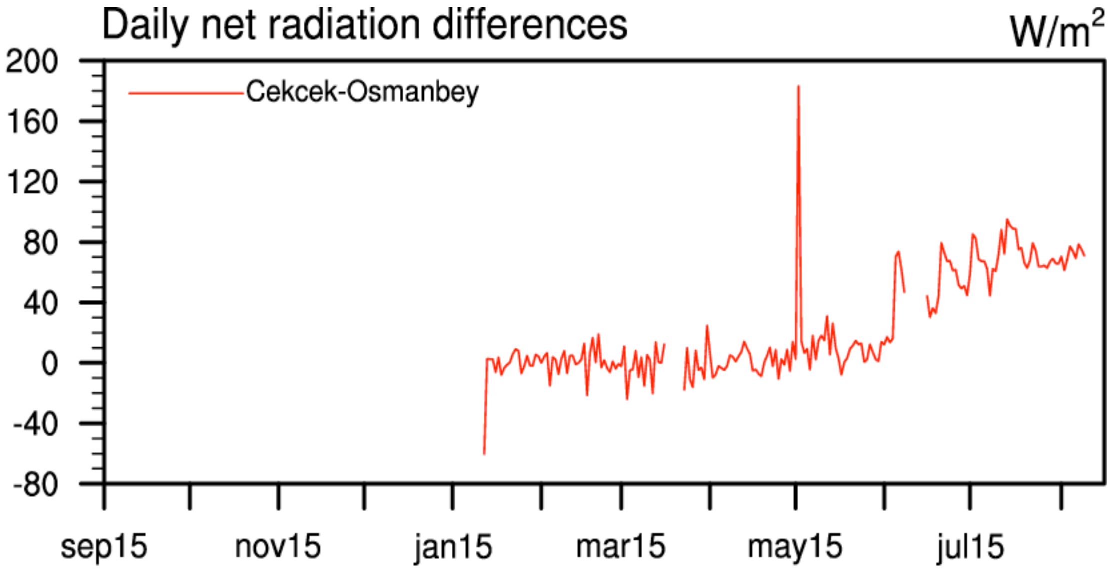

Figure.3.9 Differences in daily net radiation values for Osmanbey and Çekçek

Daily temperature values are represented in the Figure.3.10. Similar to the insolation values, temperature also peaks in summer and gets lower in winter months. Like the difference in net radiation values, temperature is also different in Osmanbey and Çekçek site from June to the end (Figure.3.11 and Figure.3.12). It is clear that there is more heat on the air in Osmanbey area comparing to Çekçek (Figure.3.13).

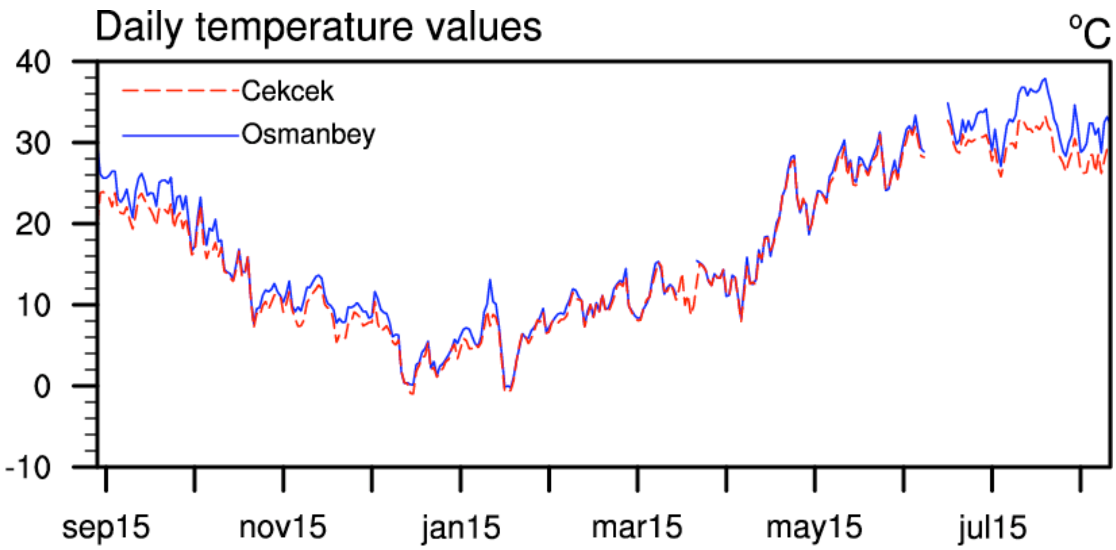

Figure.3.10 Daily averaged temperature values for Osmanbey and Çekçek

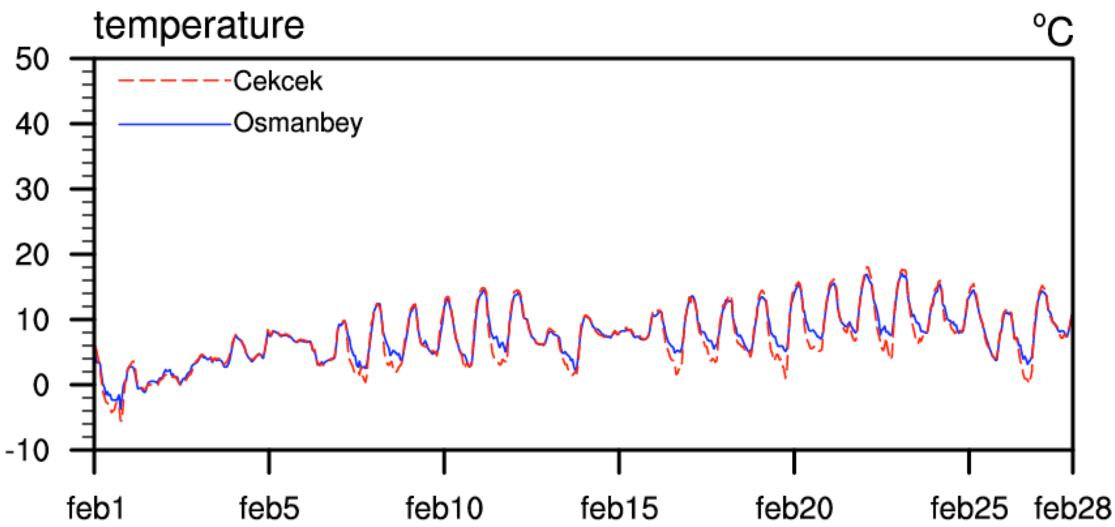

Figure.3.11 Hourly temperature data for Osmanbey and Çekçek (February)

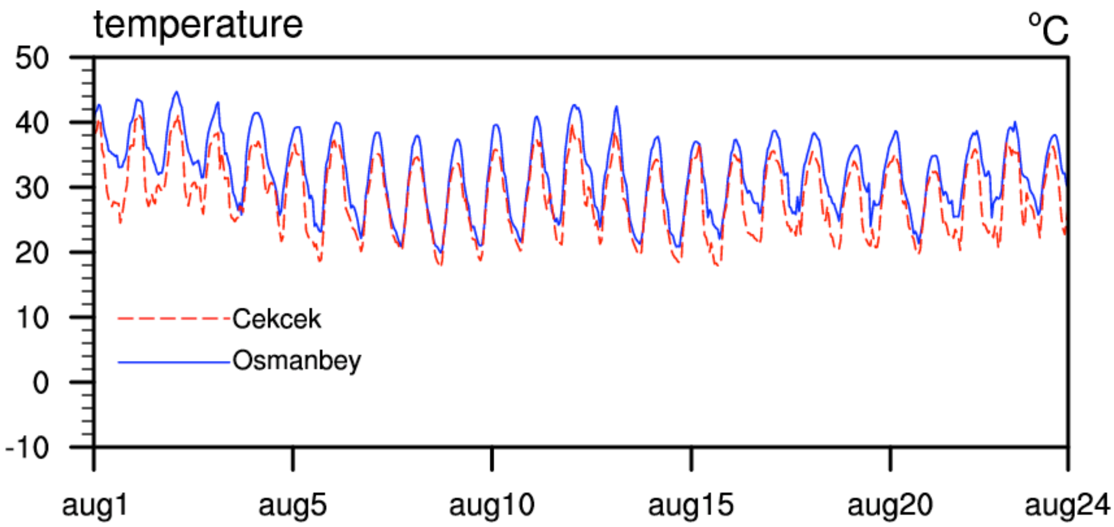

Figure.3.12 Hourly temperature data for Osmanbey and Çekçek (August)

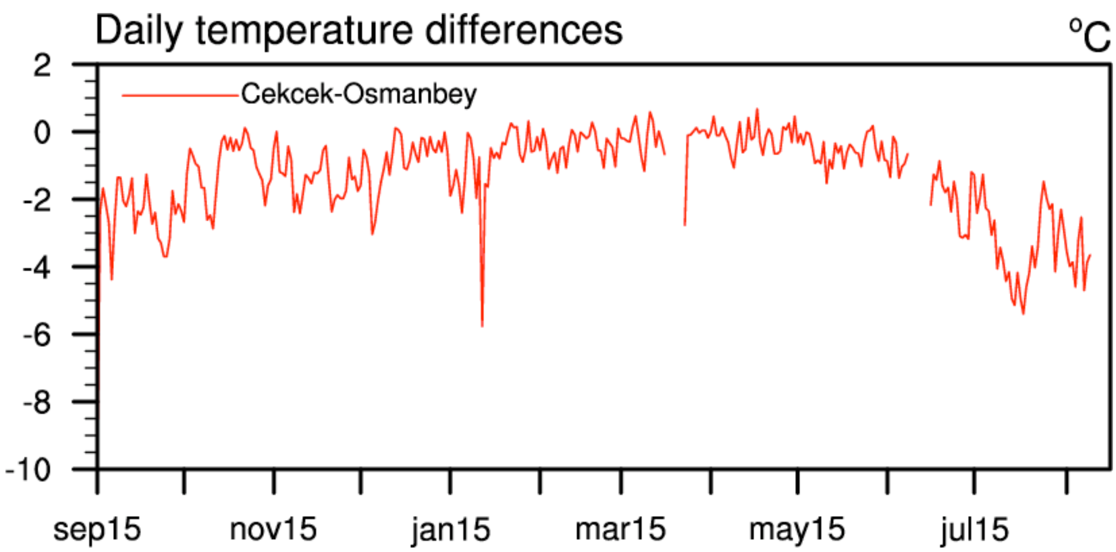

Figure.3.13. Differences in daily temperature values for Osmanbey and Çekçek

In the relative humidity values, there is a similar pattern in both experimental sites. Only after June, there is a positive difference in Çekçek comparing to Osmanbey (see figures 3.14, 3.15, 3.16 and 3.17 below).

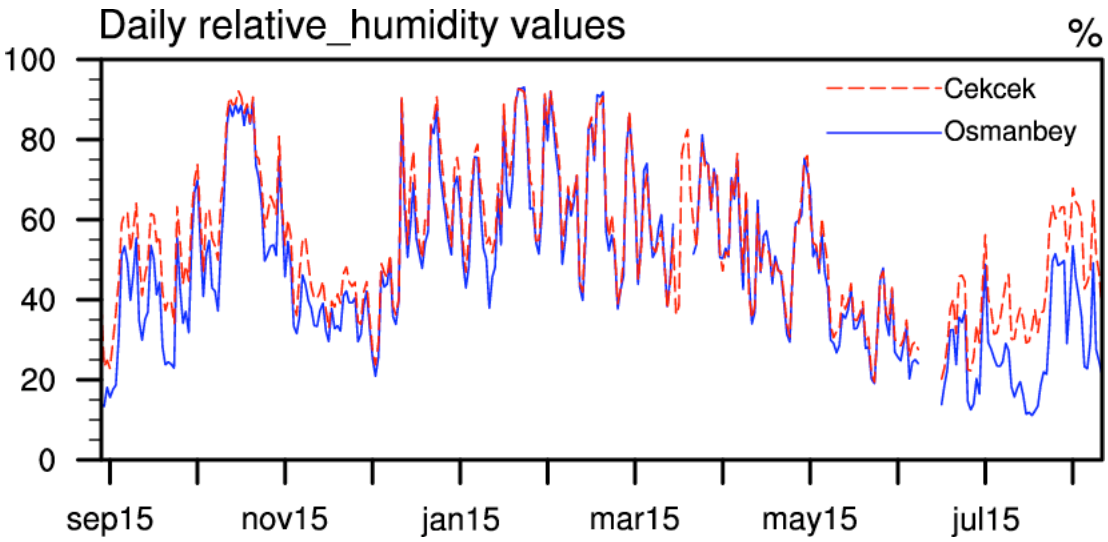

Figure.3.14 Daily averaged relative humidity values for Osmanbey and Çekçek

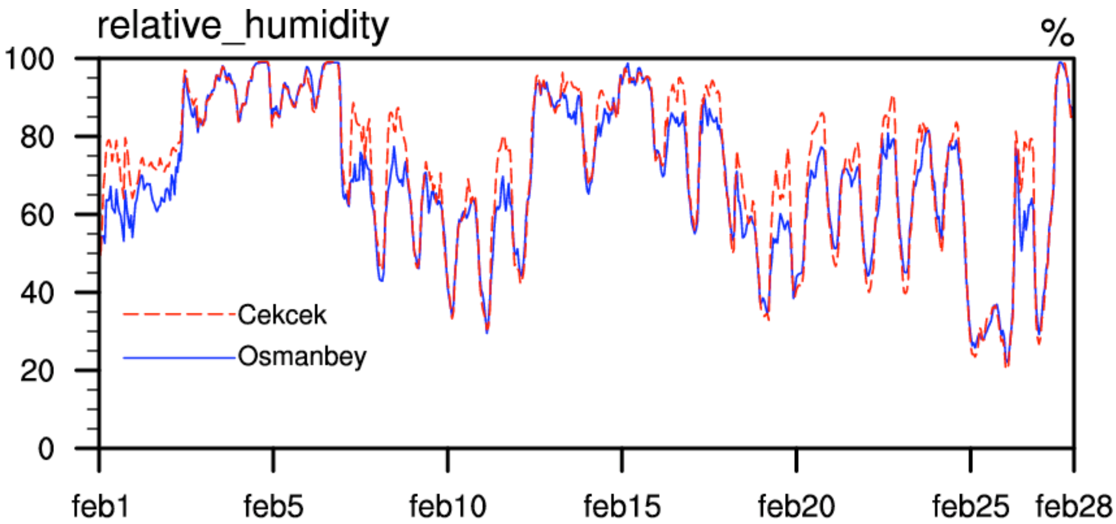

Figure.3.15 Hourly relative humidity data for Osmanbey and Çekçek (February)

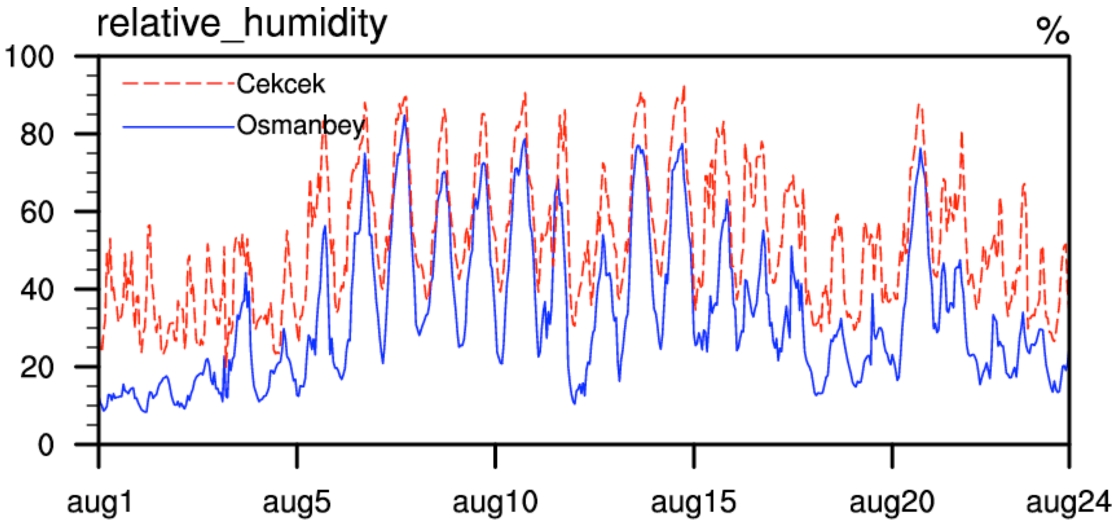

Figure.3.16 Hourly relative humidity data for Osmanbey and Çekçek (August)

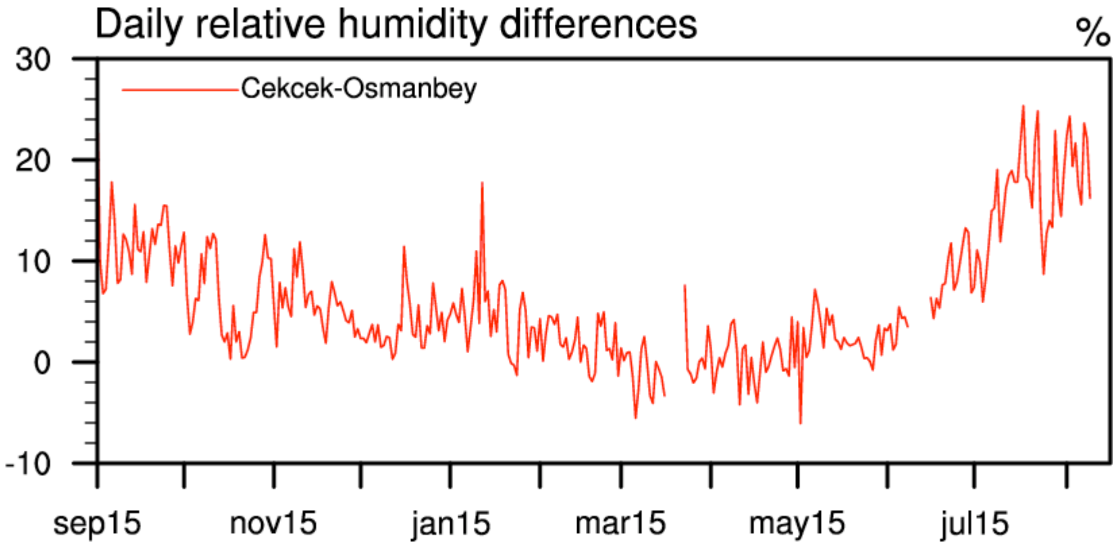

Figure.3.17 Differences in daily relative humidity values for Osmanbey and Çekçek

To represent the differences in Osmanbey and Çekçek more clearly, dew point temperatures are calculated for each site and the plots are shown below. Since dew point temperature includes both temperature and humidity values, these plots are kind of more focused examination of the differences. As it is seen in the Figure.3.18, the dew point temperature values also differ mostly in summer months for both sites. A more closed look in February (Figure.3.19) and August (Figure.3.20) supports this incident. For the overall differences, the Figure.3.21 represents the general idea.

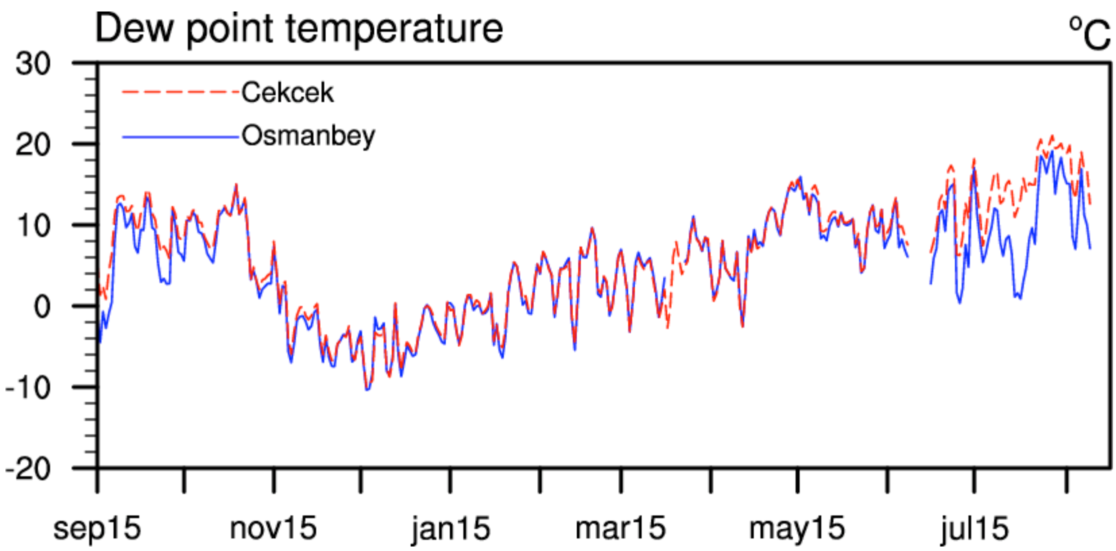

Figure.3.18 Daily averaged dew point temperature values for Osmanbey and Çekçek

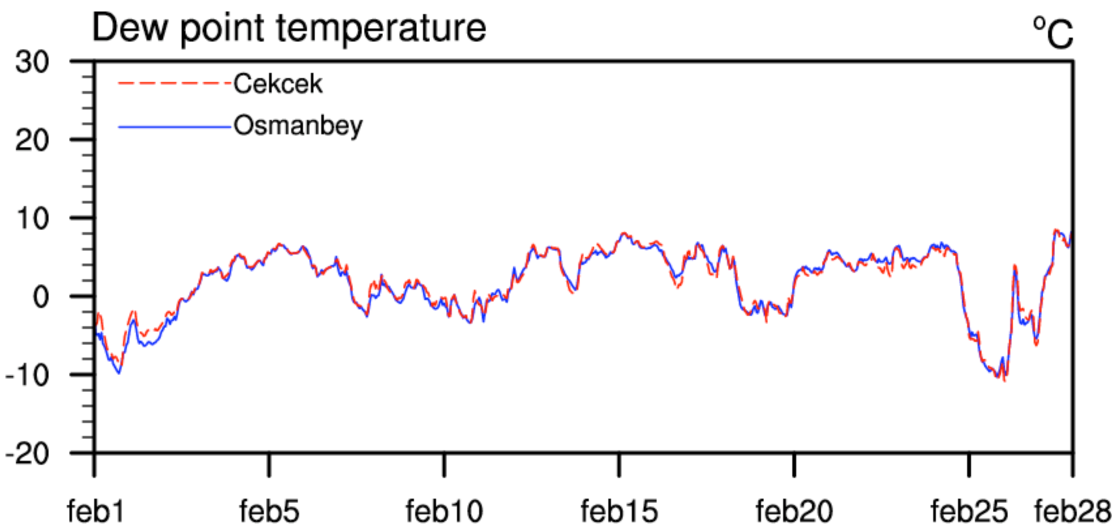

Figure.3.19 Hourly dew point temp. values for Osmanbey and Çekçek (February)

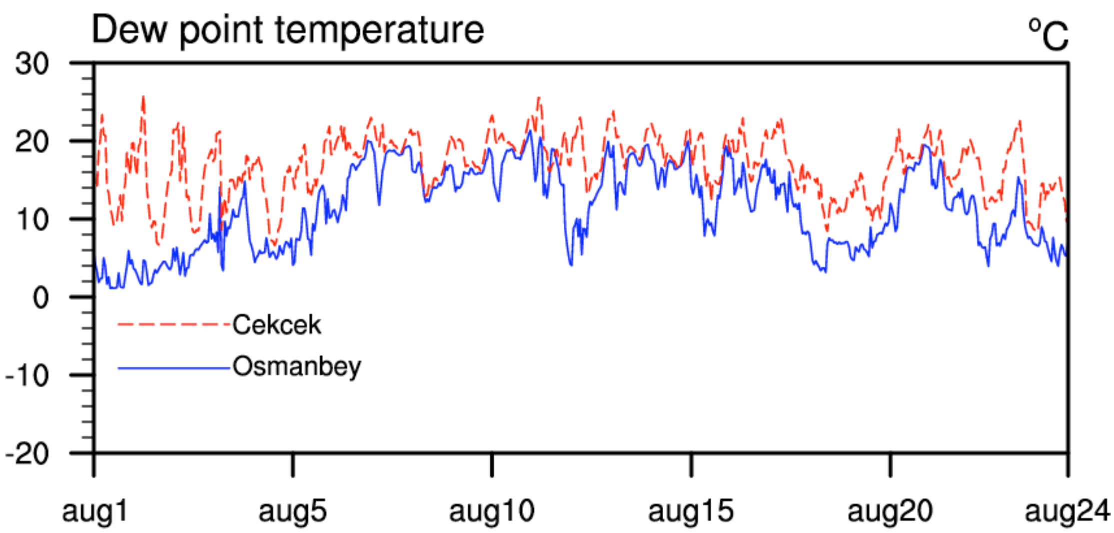

Figure.3.20 Hourly dew point temp. values for Osmanbey and Çekçek (August)

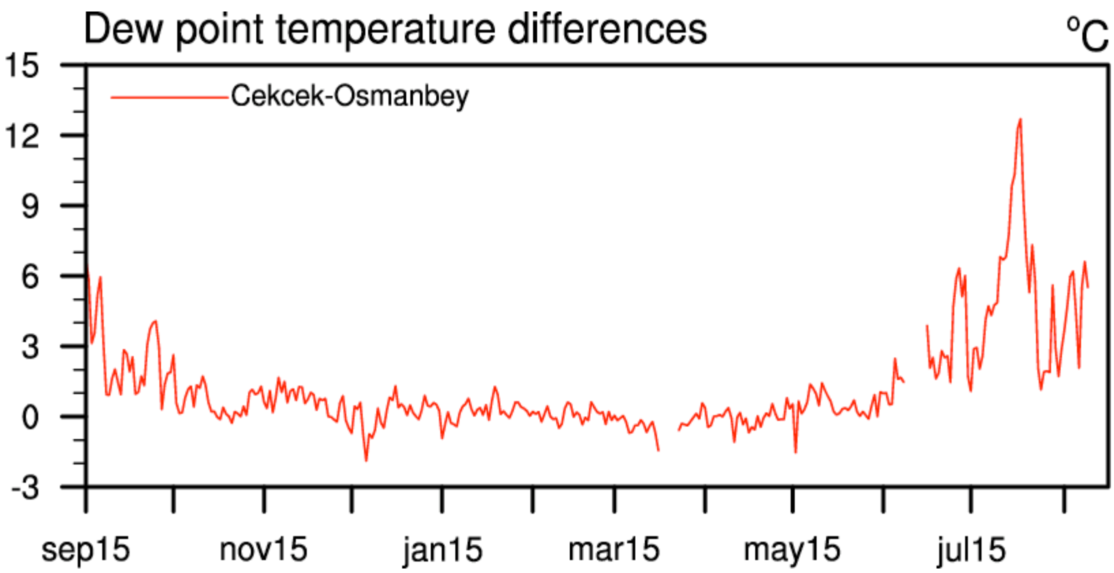

Figure.3.21 Differences in daily dew point temp. values for Osmanbey and Çekçek

The figure below (Figure.3.22) shows the wind speed values. Through close examination it can be seen that there is higher wind speed values in Osmanbey site in summer months (Figure.3.24) and in winter both sites seem to have similar wind speeds (Figure.3.23). Figure.3.25 shows the all year wind speed differences for Osmanbey and Çekçek.

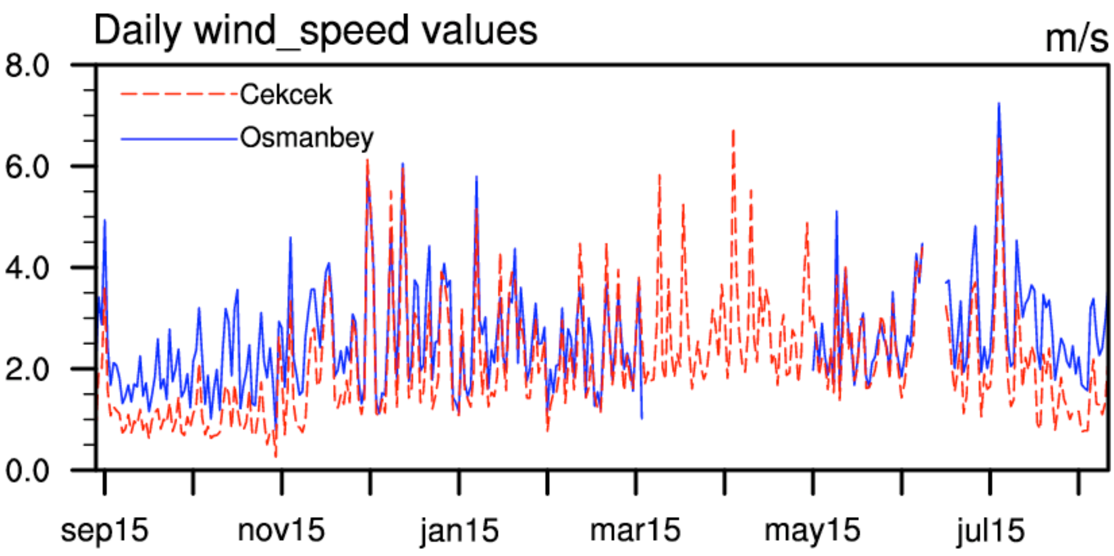

Figure.3.22 Daily averaged wind speed values for Osmanbey and Çekçek

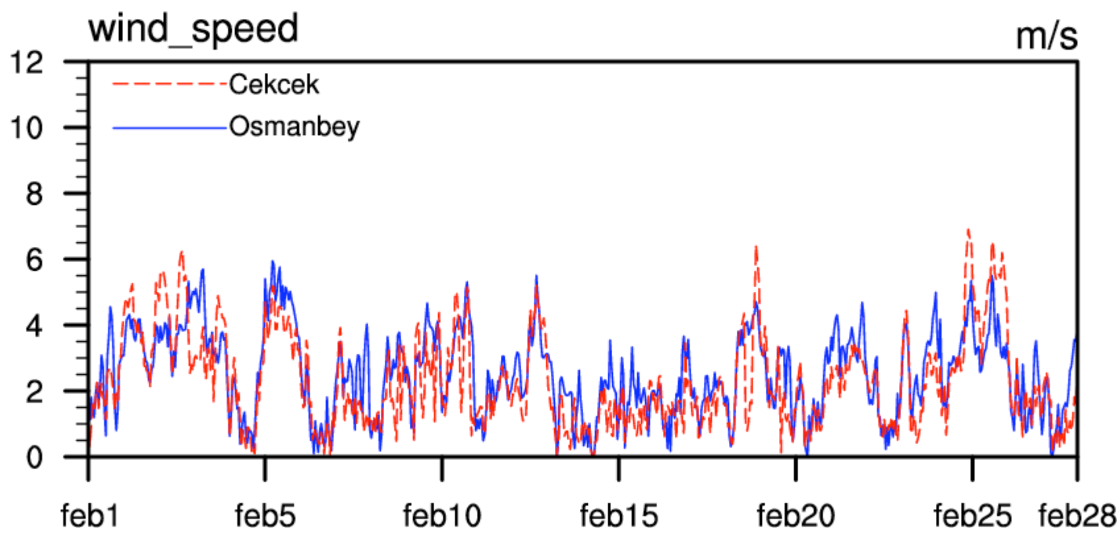

Figure.3.23 Hourly wind speed data for Osmanbey and Çekçek (February)

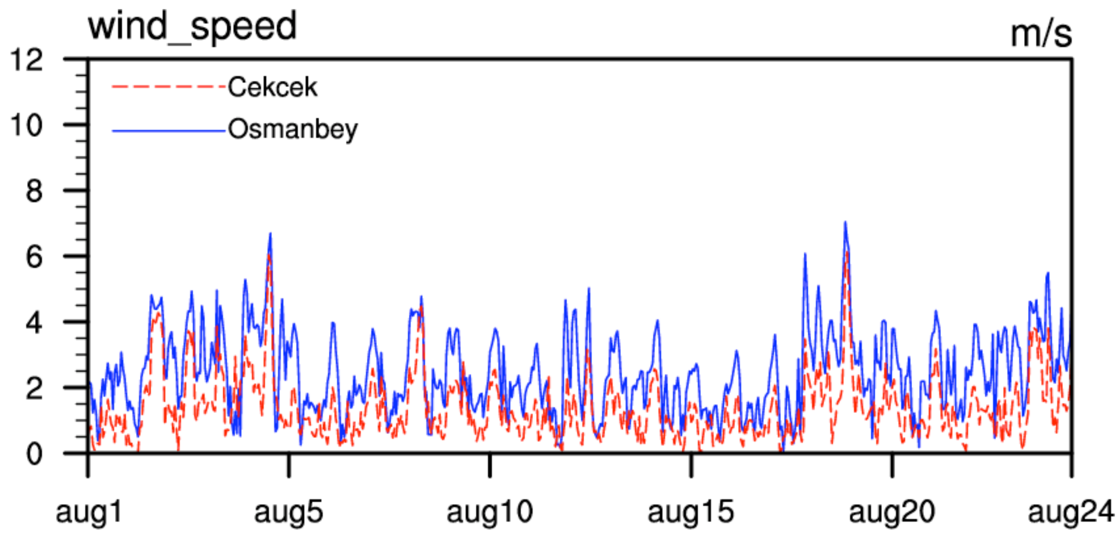

Figure.3.24 Hourly wind speed data for Osmanbey and Çekçek (August)

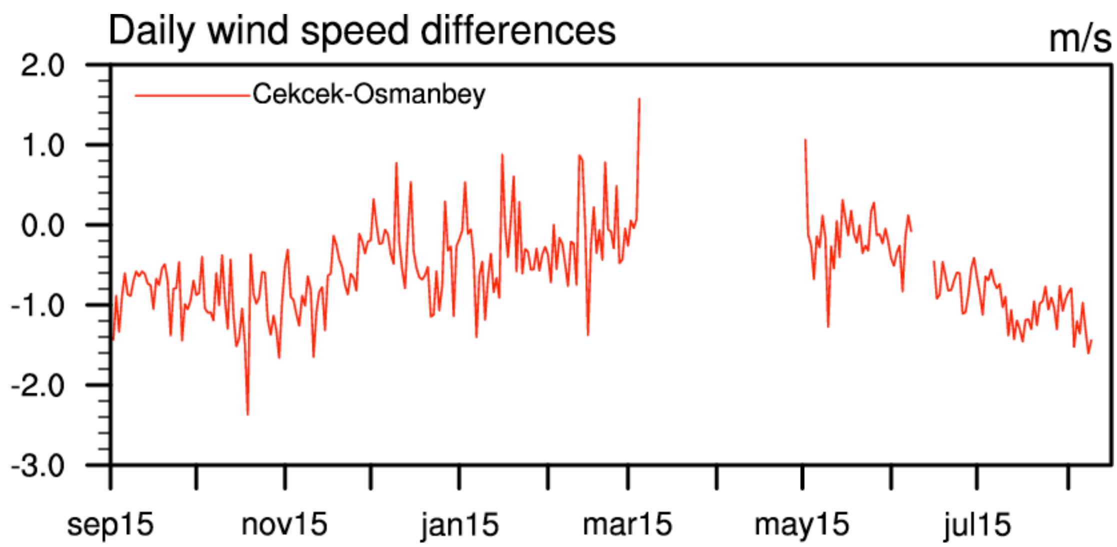

Figure.3.25 Differences in daily wind speed values for Osmanbey and Çekçek

As seen in the figures below (Figure.3.26 and Figure.3.27), wind rose plots show the prevailing wind directions for both of the sites. Most of the time, there are northerly winds and the directions are similar for each site.

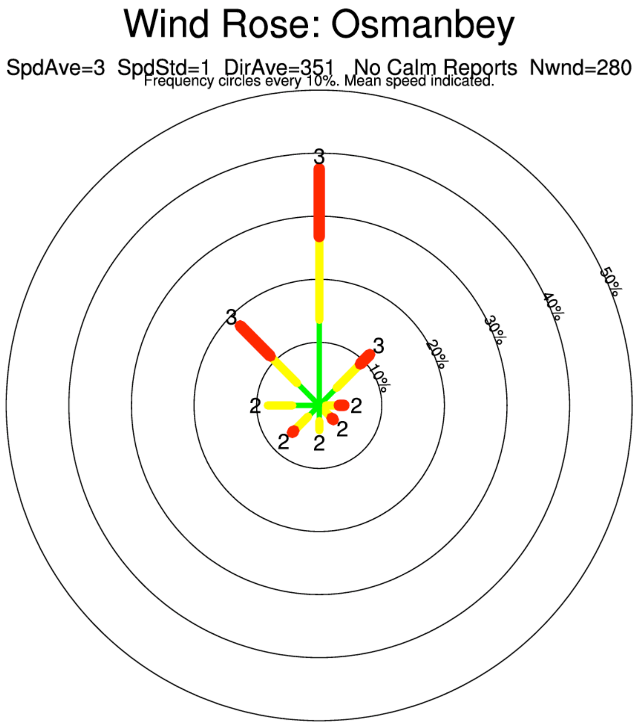

Figure.3.26 Wind rose for Osmanbey

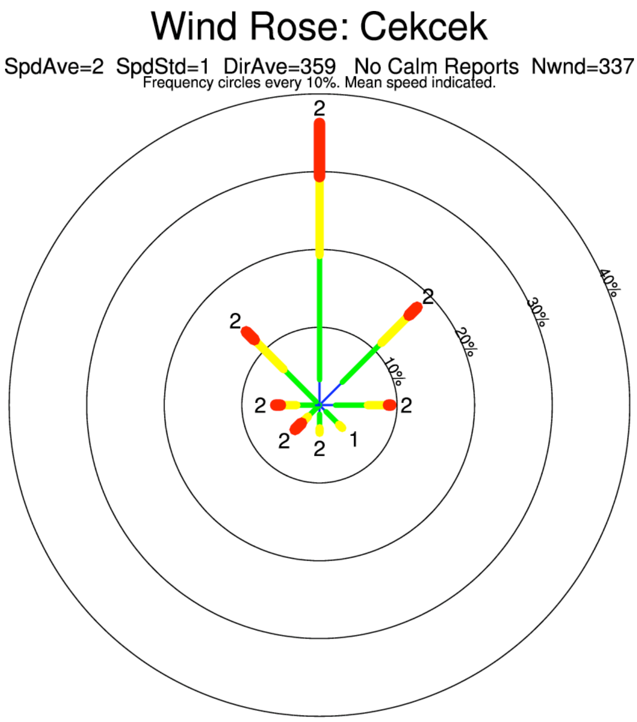

Figure.3.27 Wind rose for Çekçek

The figures above show all the gathered meteorological data for Osmanbey and Çekçek. Considering the daily changes in surface heat processes and evapotranspiration activities, diurnal cycles are represented in the following figures. For better understanding the time periods when there is a difference, seasonally averaged diurnal cycles for insolation, net radiation, temperature, relative humidity, wind speed and total precipitation are plotted and panelled below. As demonstrated in the previous figures months in autumn (Figure.3.28), winter (Figure.3.29) and spring (Figure.3.30) show little differences; but in summer months dissimilarities are more obvious (Figure.3.31).

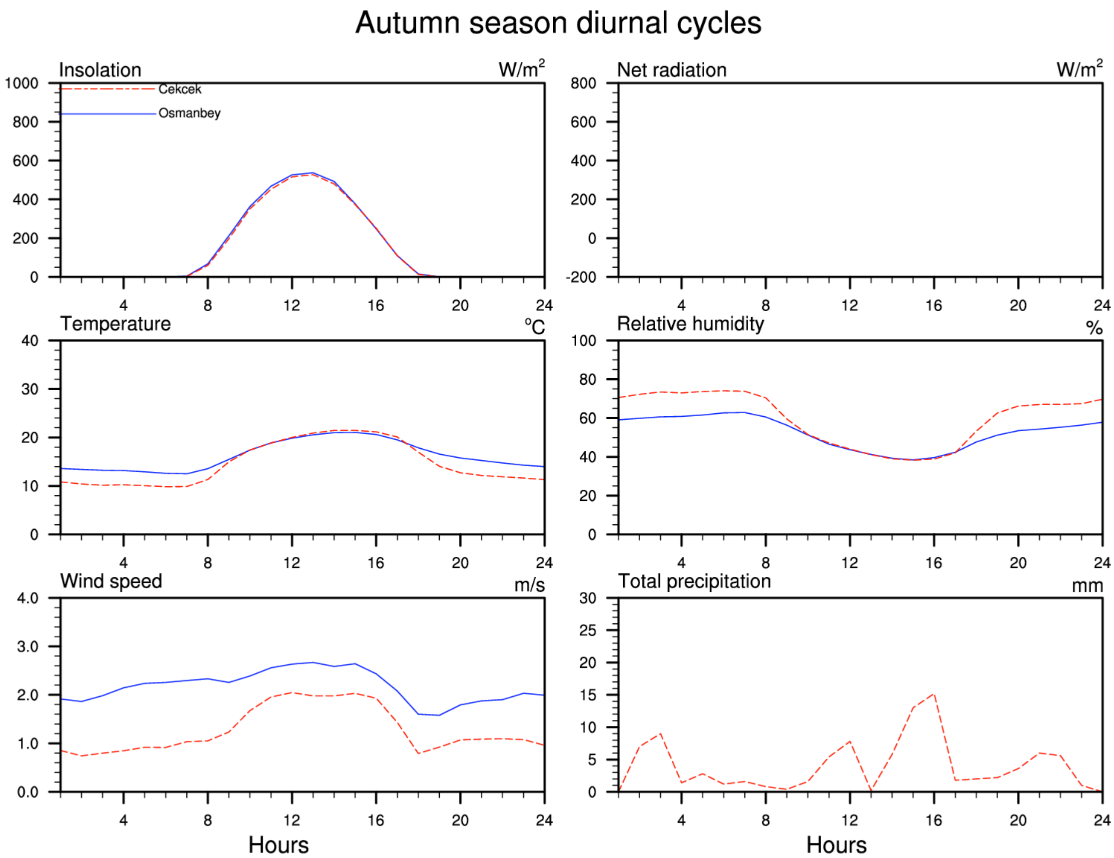

Figure.3.28 Panel plot for autumn season diurnal cycles in Osmanbey and Çekçek

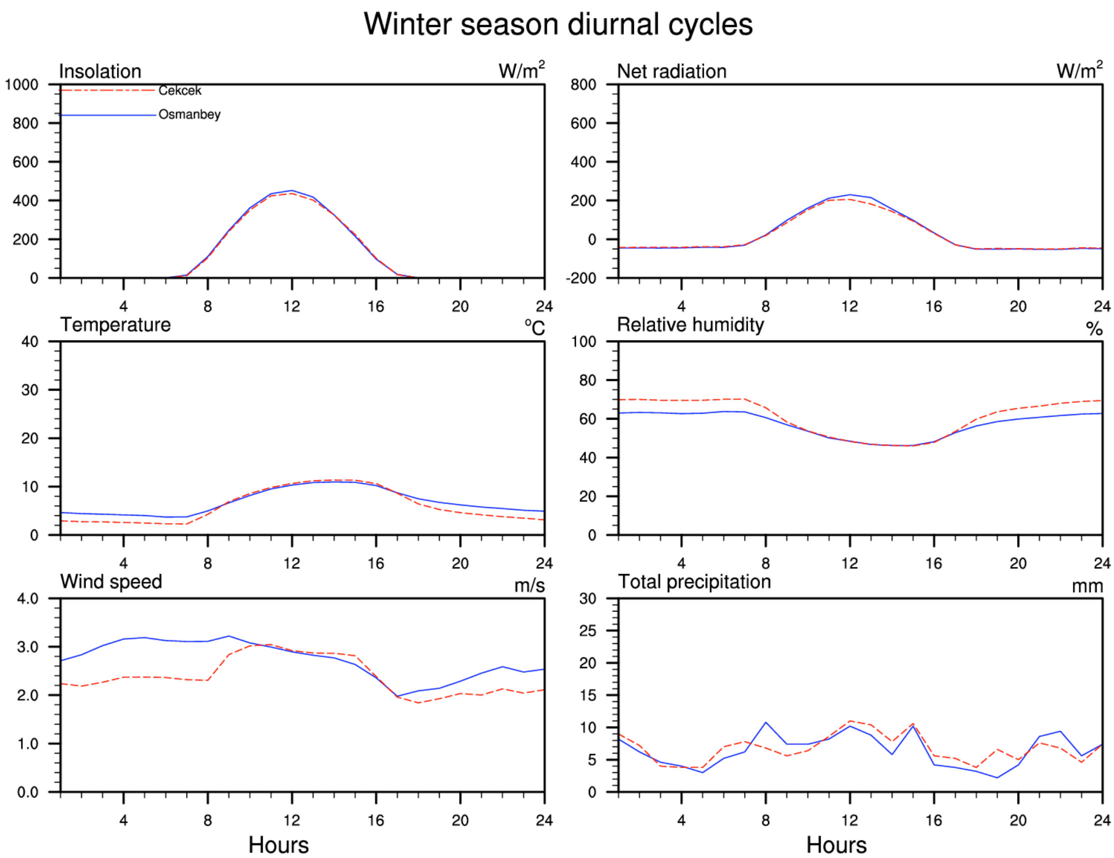

Figure.3.29 Panel plot for winter season diurnal cycles in Osmanbey and Çekçek

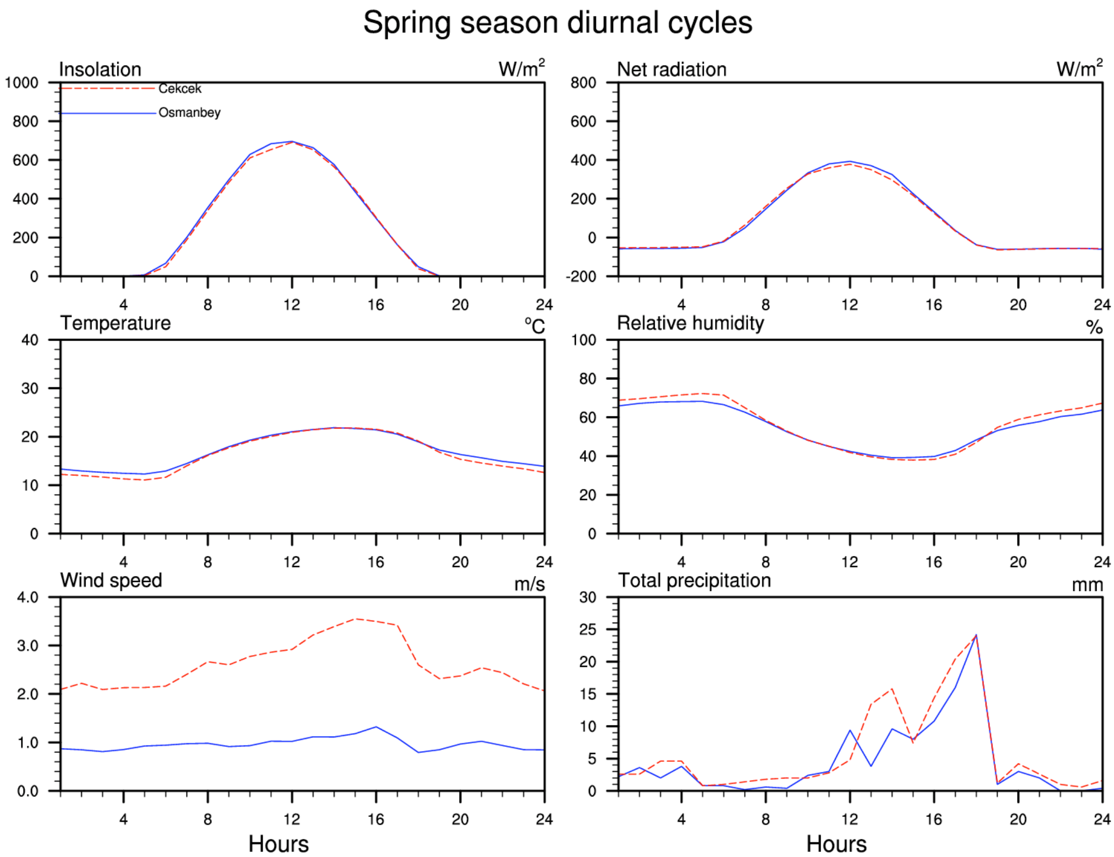

Figure.3.30 Panel plot for spring season diurnal cycles in Osmanbey and Çekçek

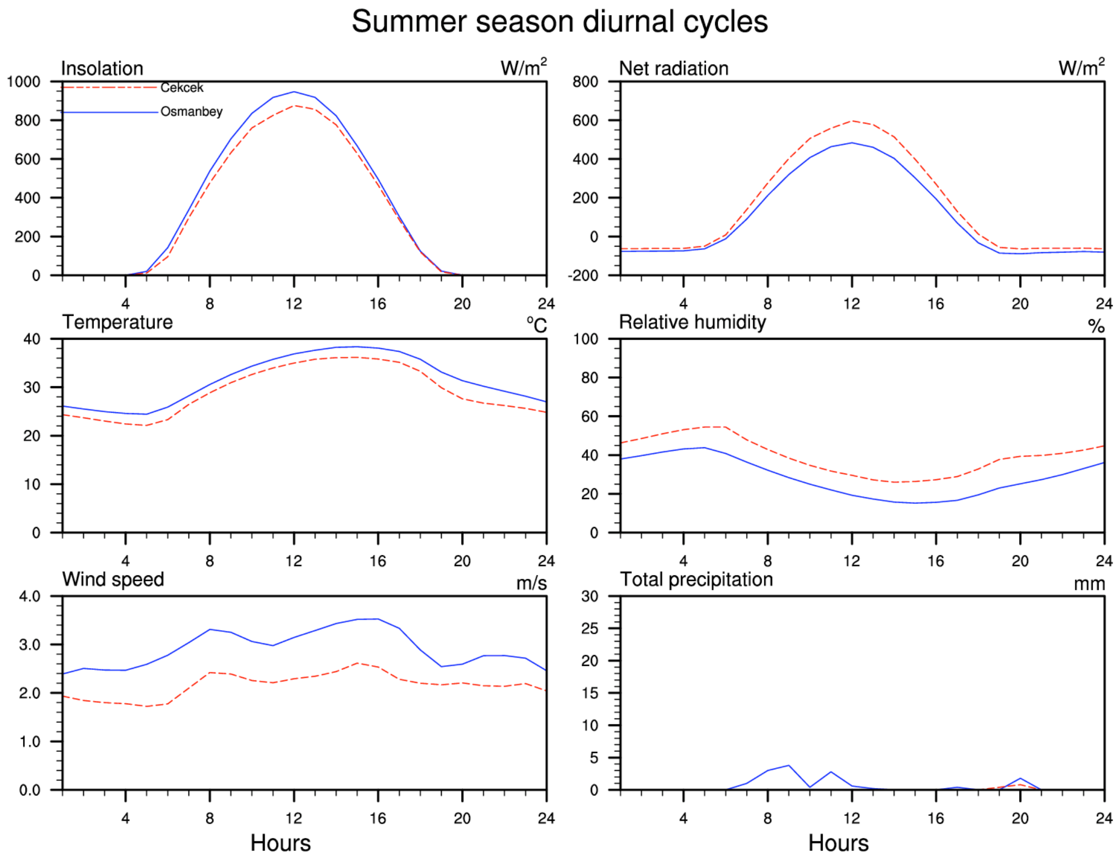

Figure.3.31 Panel plot for summer season diurnal cycles in Osmanbey and Çekçek

The sensible heat flux comparison plot (Figure.3.32) shows a similar trend except from summer months. In June and July there is a remarkable difference between Osmanbey and Çekçek areas. Sensible heat flux keeps increasing in Osmanbey; while it suddenly starts decreasing in Çekçek during June and July. The figures 3.33 and 3.34 points out the differences in January and July.

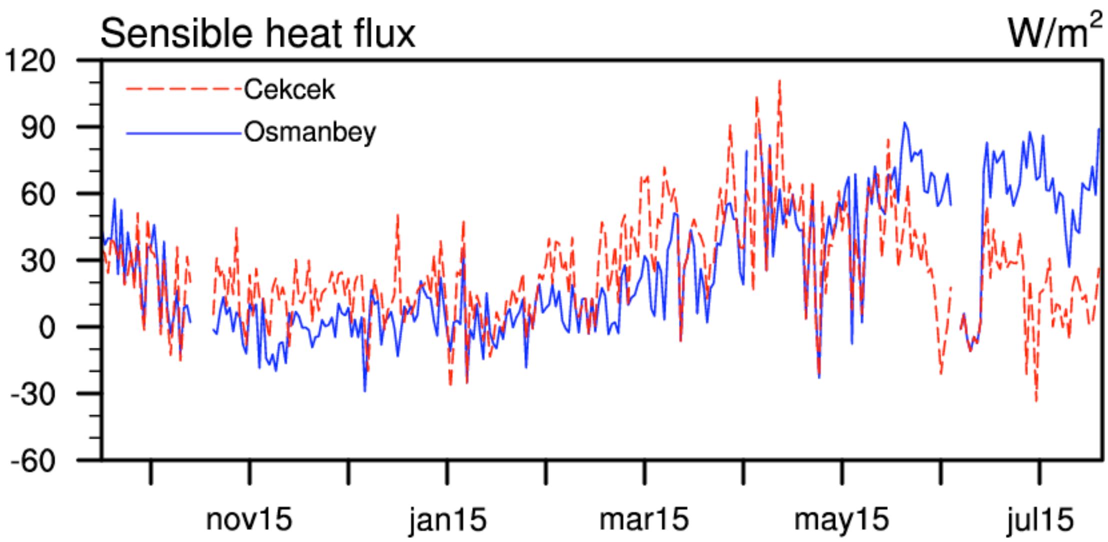

Figure.3.32 Daily averaged sensible heat flux values for Osmanbey and Çekçek

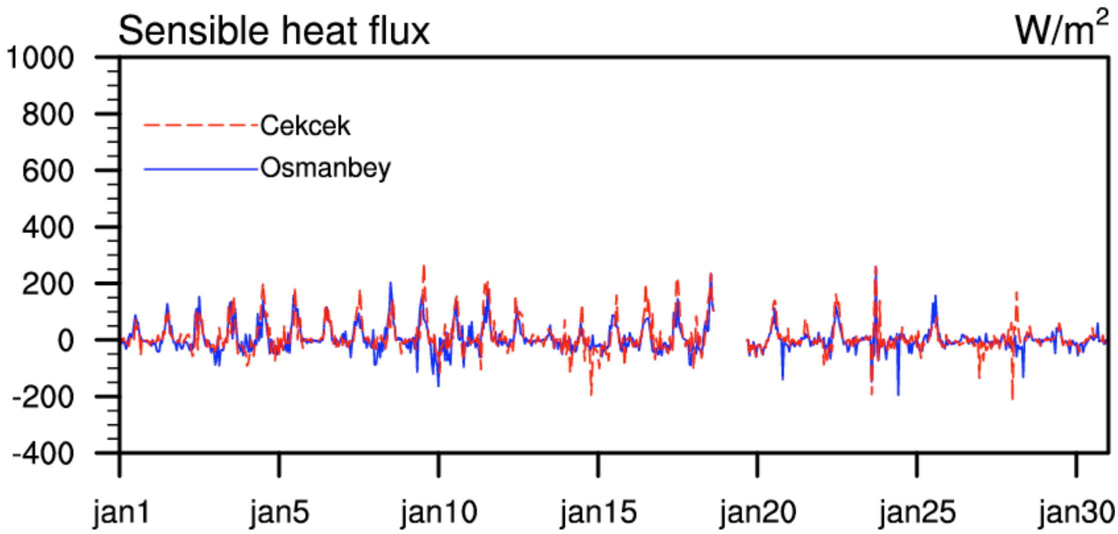

Figure.3.33 Hourly sensible heat flux data for Osmanbey and Çekçek (January)

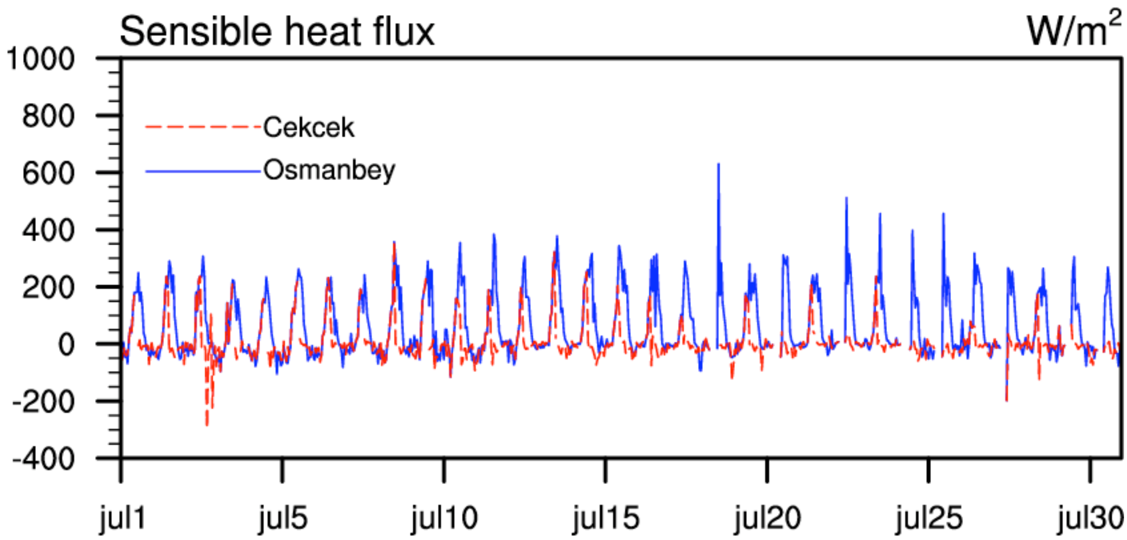

Figure.3.34 Hourly sensible heat flux data for Osmanbey and Çekçek (July)

In the previous chapters, it was pointed out that latent heat and carbon flux observations were not reliable. Therefore, they were not included in the analysis.

3.3. CLM simulation results

The modeling phase of the experiment provided the following results. Firstly the modeling performance is observed through the simulation versus observation plots and after having shown the reliability of the model, Osmanbey versus Çekçek simulations are listed in this chapter.

Modeling performance over Osmanbey area is demonstrated in the following plots. The figure below (Figure.3.35) shows the net radiation simulations for Osmanbey and it is clearly seen that most of the time period CLM and Observational results are corresponding. It was previously described that net radiation sensors are embedded to the systems in January so there is no net radiation observations before that date. If one month in summer is observed closely (Figure.3.36), the daily oscilliations can be understood more clearly.

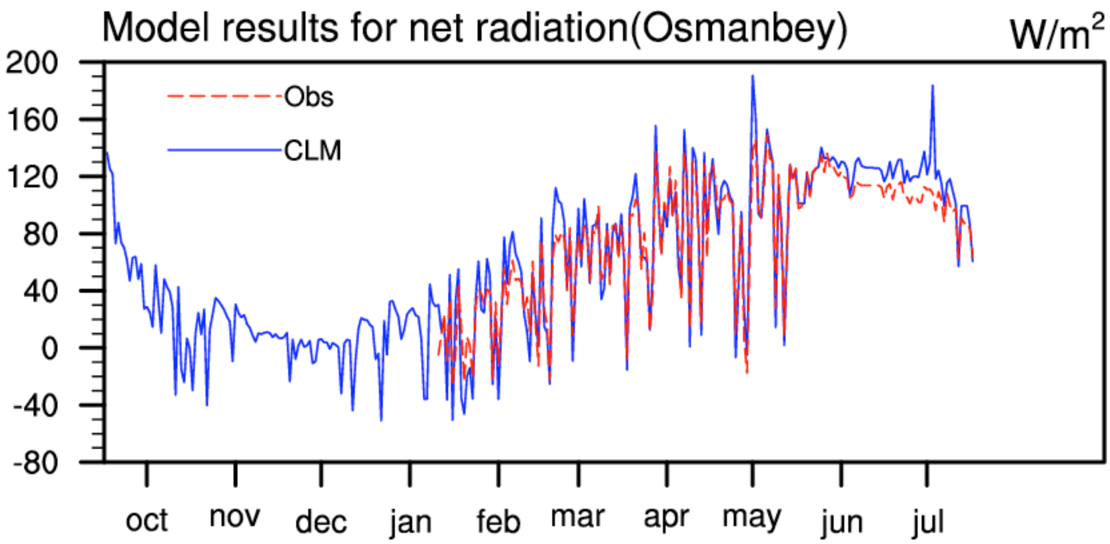

Figure.3.35 Model results for net radiation over Osmanbey (all year)

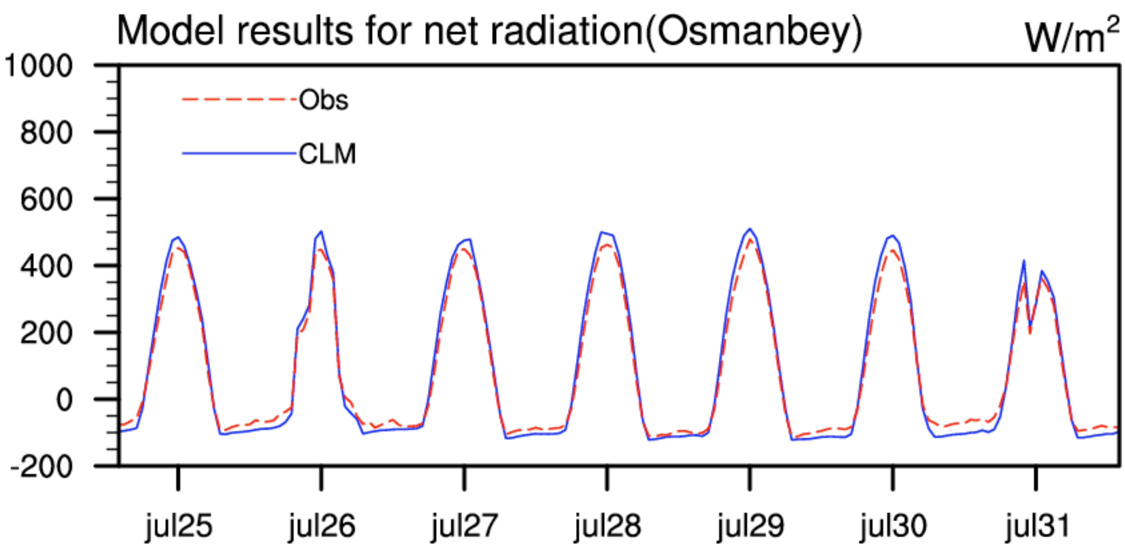

Figure.3.36 Model results for net radiation over Osmanbey (week in July)

The sensible heat flux simulations for Osmanbey reveal the following plots. The daily averaged data for the whole time period is shown in the first figure (Figure.3.37)and one week of hourly data from March is represented afterwards (Figure.3.38).

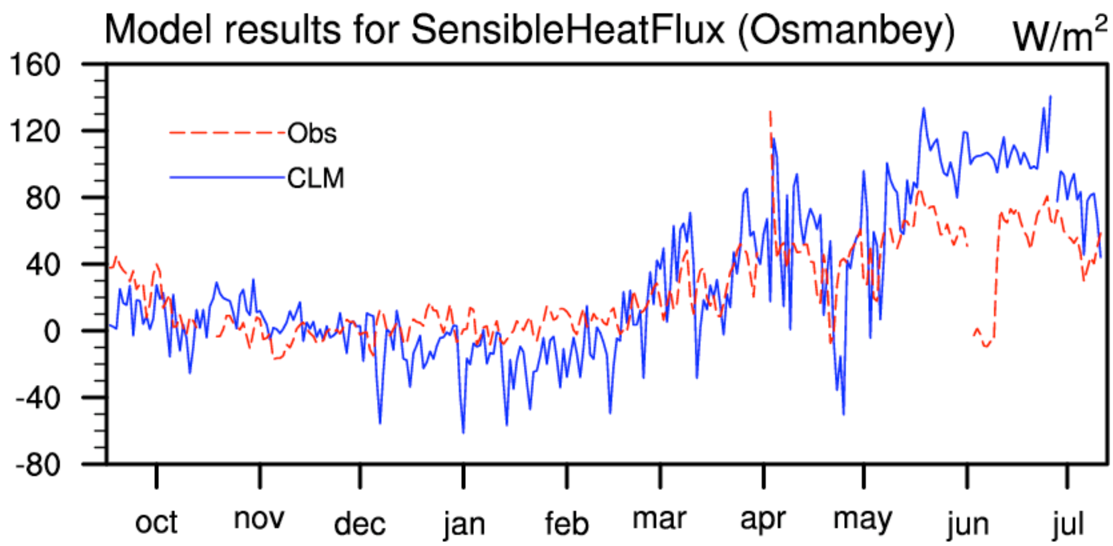

Figure.3.37 Model results for sensible heat flux over Osmanbey (all year)

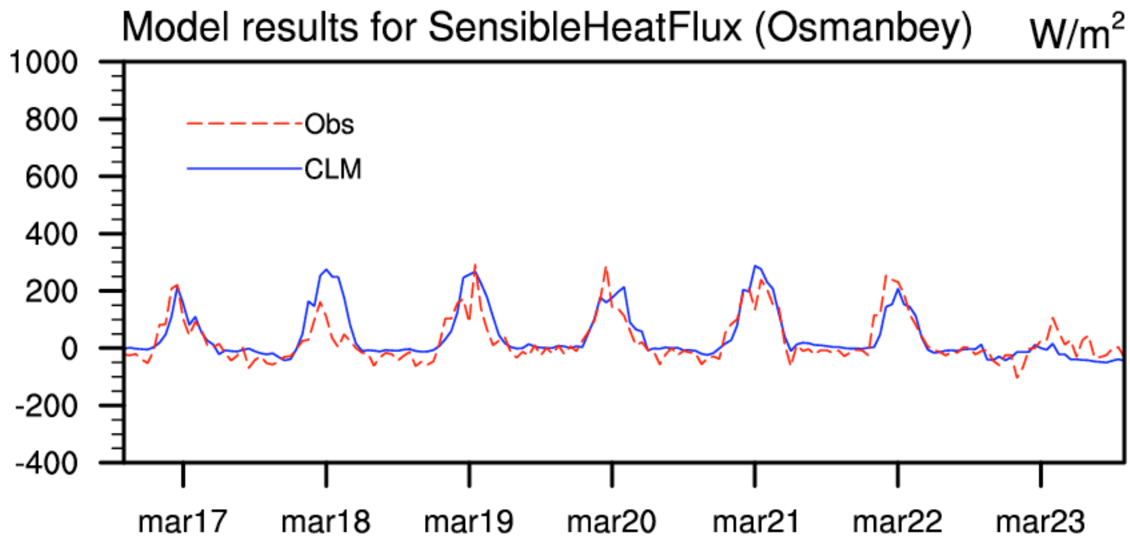

Figure.3.38 Model results for sensible heat flux over Osmanbey (week in March)

By showing the model performance over Osmanbey area, its time to show the same results for Çekçek site.

The figures below show the net radiation simulations over Çekçek area. The whole year, daily averaged data plot (Figure.3.39) and one week of hourly data plot (Figure.3.40) point out the model reliability over Çekçek site.

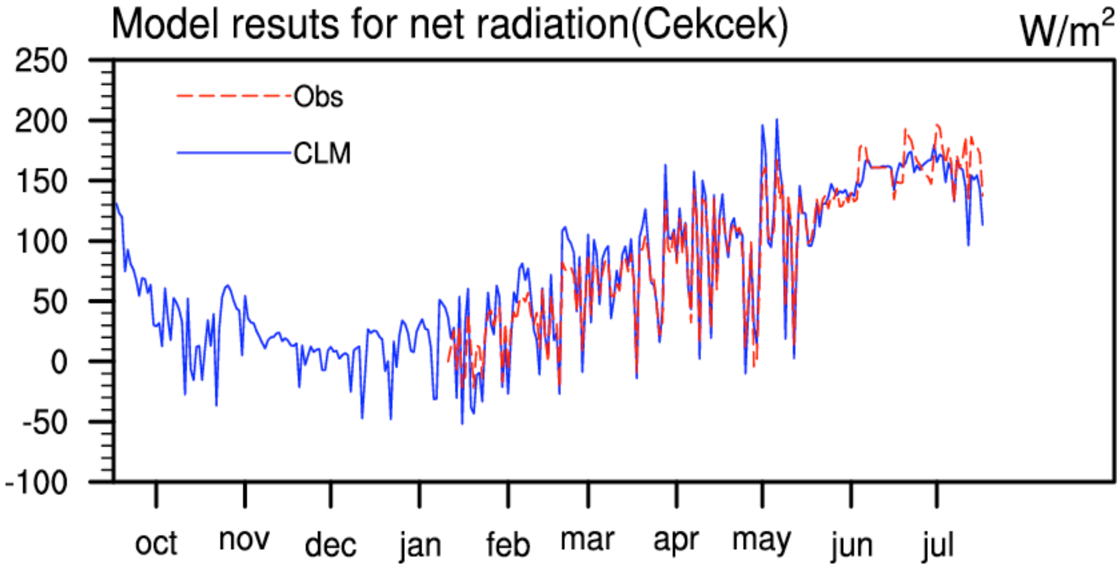

Figure.3.39 Model results for net radiation over Çekçek (all year)

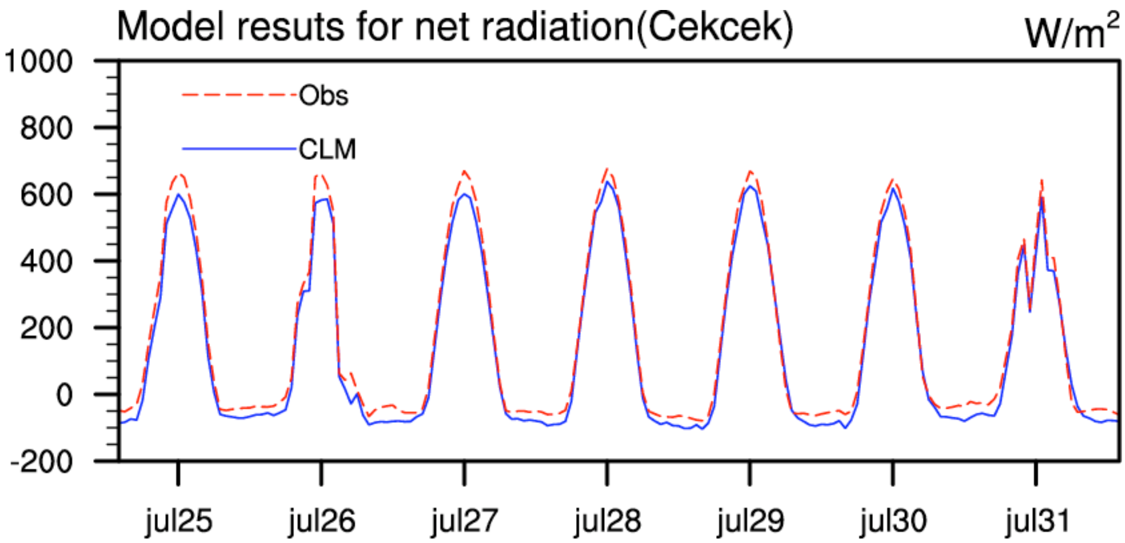

Figure.3.40 Model results for net radiation over Çekçek (week in July)

For the sensible heat flux simulations the following figure (Figure.3.41) respresents the CLM versus observational data. It is visible that the CLM is capturing the main pattern throughout the time period except from summer. In summer the simulations show a positive surplus in sensible heat flux values comparing to the observational results. This dissimilarity is pointed out in the discussions section afterwards. As it is described, the weekly plot (Figure.3.42) of hourly data in March proves the model performance over Çekçek area for sensible heat flux.

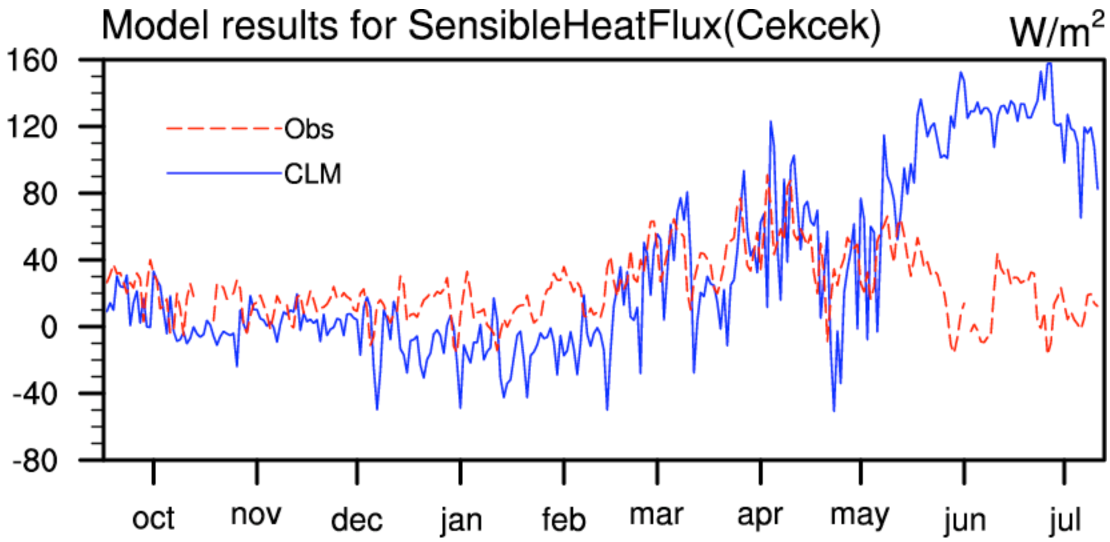

Figure.3.41 Model results for sensible heat flux over Çekçek (all year)

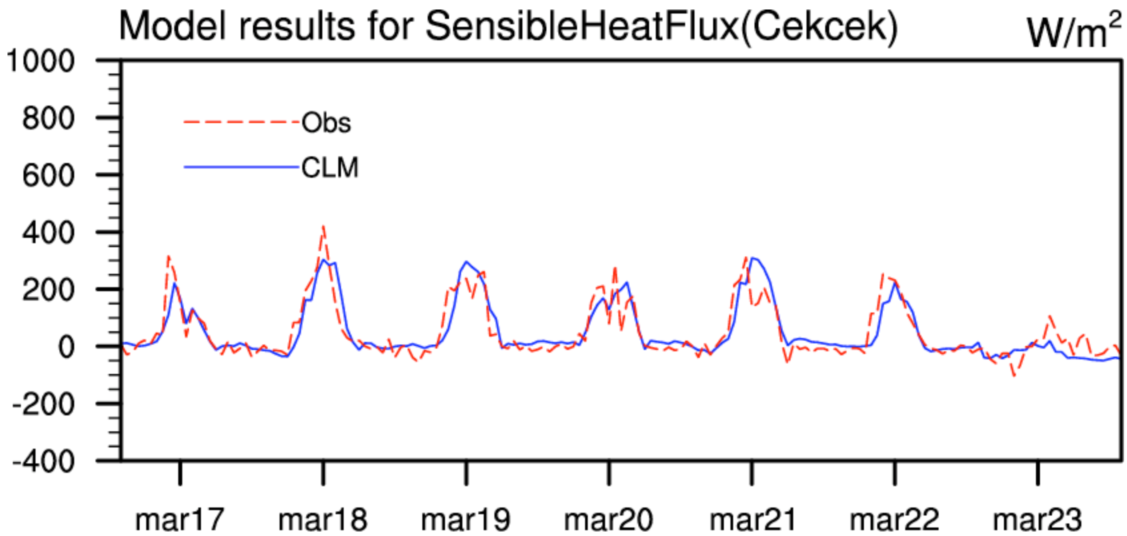

Figure.3.42 Model results for sensible heat flux over Çekçek (week in March)

With demonstrating the model performance by showing CLM versus observation plots, the differences in simulation results over Osmanbey and Çekçek are shown in the following pages. Under the light of reliability plots, the comparison plots signify the discussed dissimilarities for the experiment.

In the net radiation comparison plot below (Figure.3.43), it is obvious that most of the time period the model gave similar results for Osmanbey and Çekçek; but in summer there is more net radiation available in Çekçek area, as supporting the observational results shown in the previous pages.

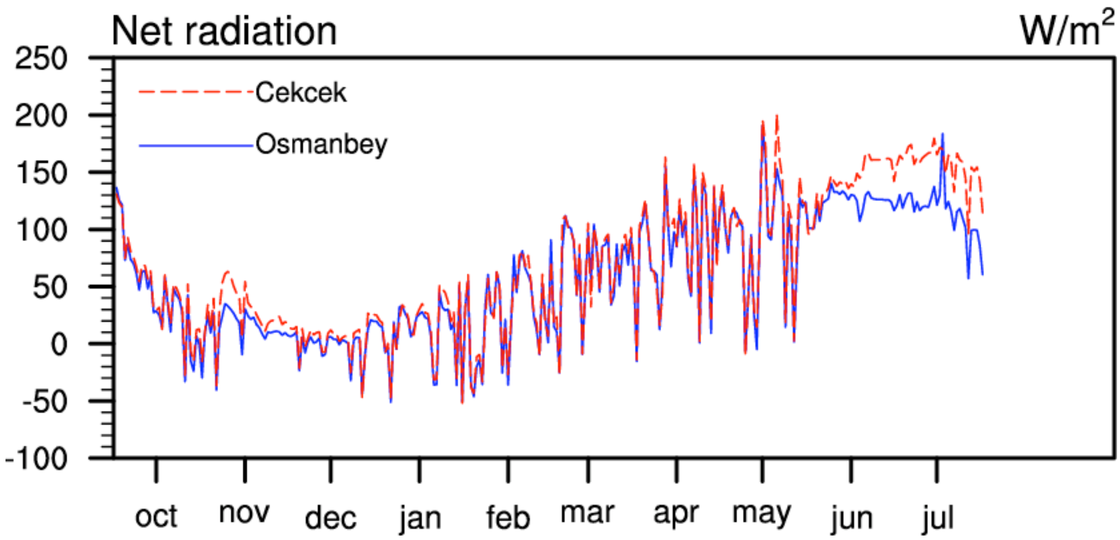

Figure.3.43 Model results for net radiation for Osmanbey and Çekçek

Like it was pointed out before, the sensible heat flux simulations over Çekçek area are representing some unexpected results in summer. If the figure below (Figure.3.44) is examined, there is more sensible heat flux in Çekçek area during the summer months. For better understanding of this case, please see the discussions part.

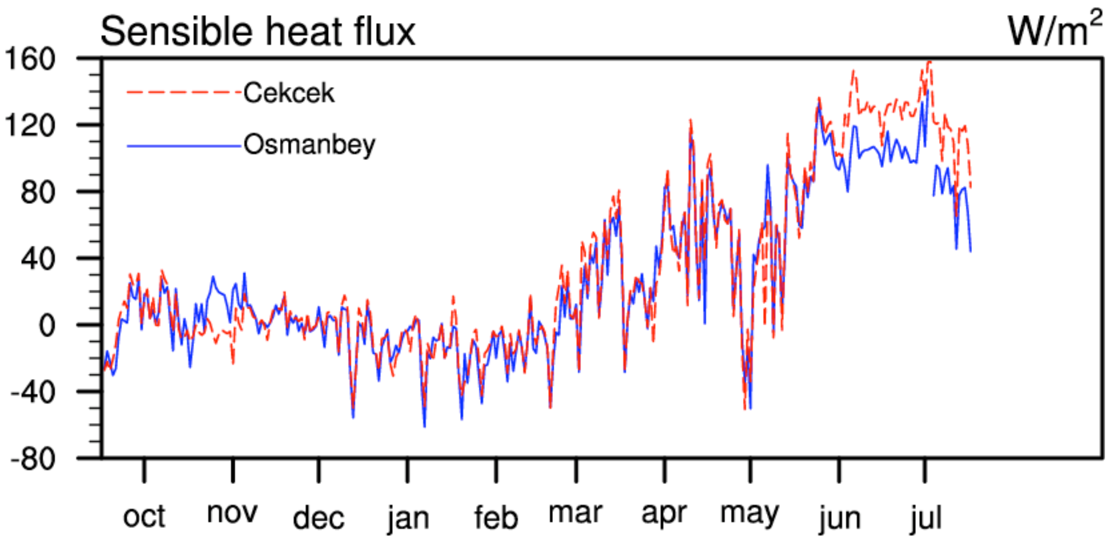

Figure.3.44 Model results for sensible heat flux for Osmanbey and Çekçek

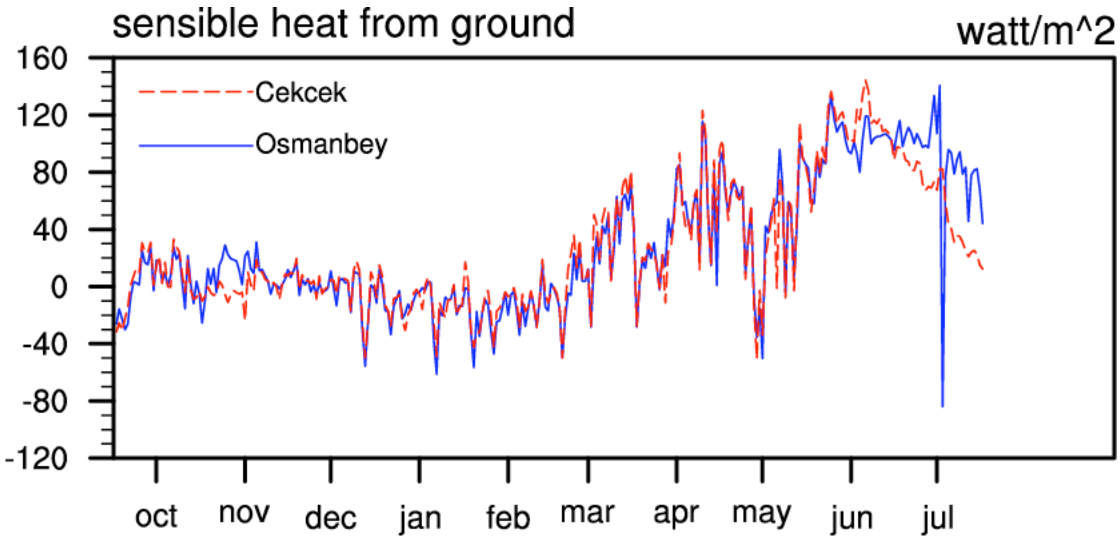

Figure.3.45 Model results for sensible heat flux from ground for Osmanbey and Çekçek

In Figure 3.45 it is shown that the produced sensible heat flux from Çekçek ground is decreasing in summer. Having shown the sensible heat from ground, the other component of total sensible heat flux, sensible heat from vegetation, is given in Figure.3.46.

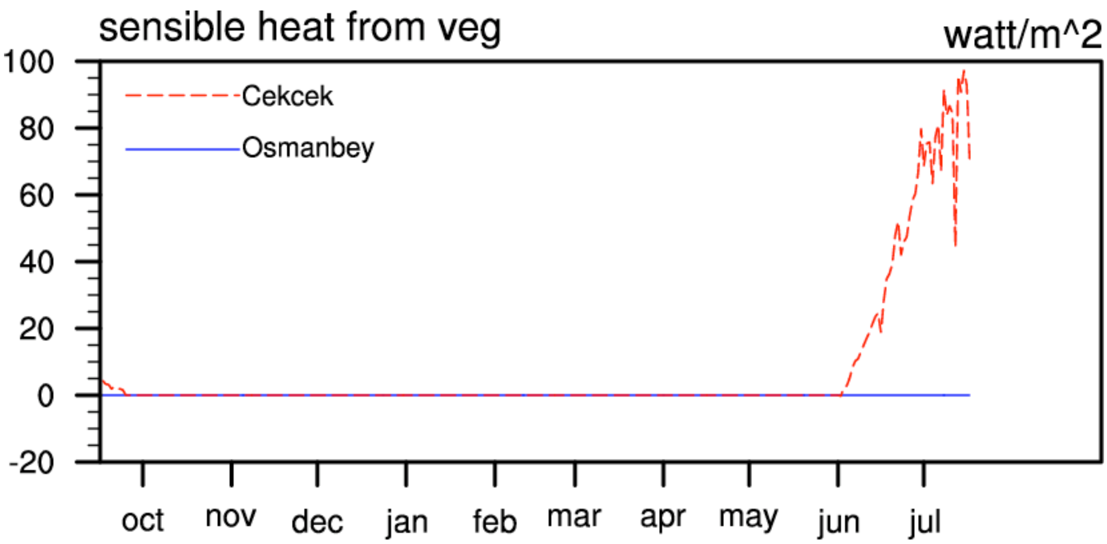

Figure.3.46 Model results for sensible heat flux from vegetation for Osmanbey and Çekçek

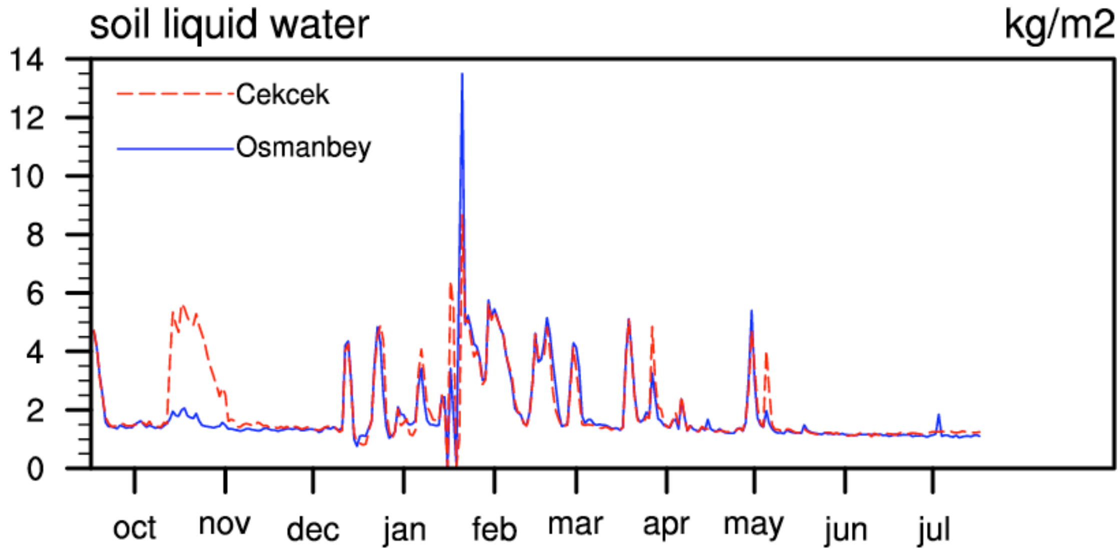

Figure.3.47 Model results for soil liquid water in the first soil layer for Osmanbey and Çekçek

In the figures 3.47 and 3.48 the available liquid water in different soil layers are represented. While Figure.3.47 is showing the first soil layer (the closest layer to the surface), Figure.3.48 shows the second soil layer. Since the other seven soil layers have a more smooth but similar results, they are not included here.

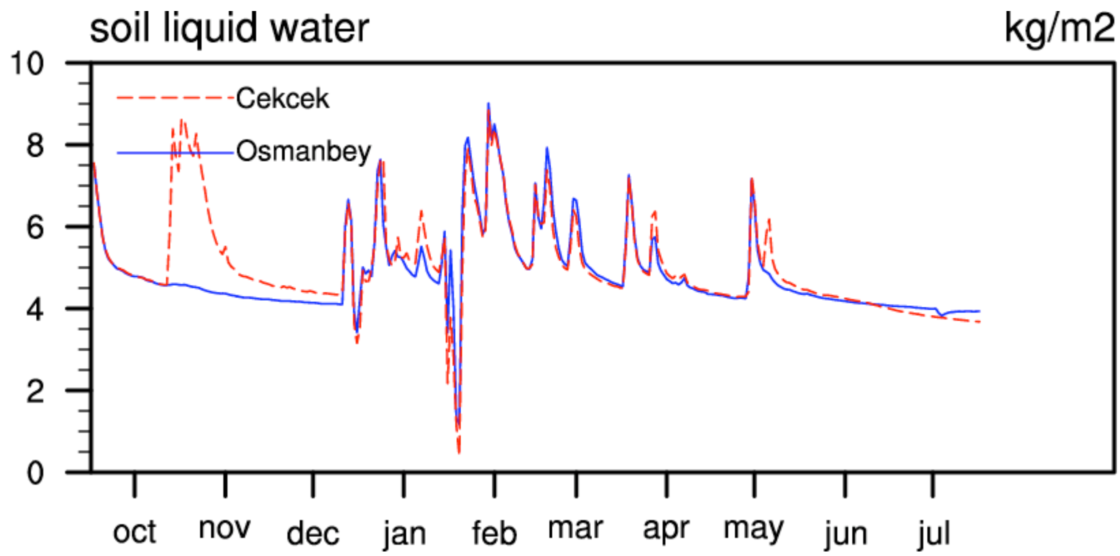

Figure.3.48 Model results for soil liquid water in the second soil layer for Osmanbey and Çekçek

Solar radiation and its components are given in the following figures. The Figure.3.49 shows the reflected solar radiation for both sites.

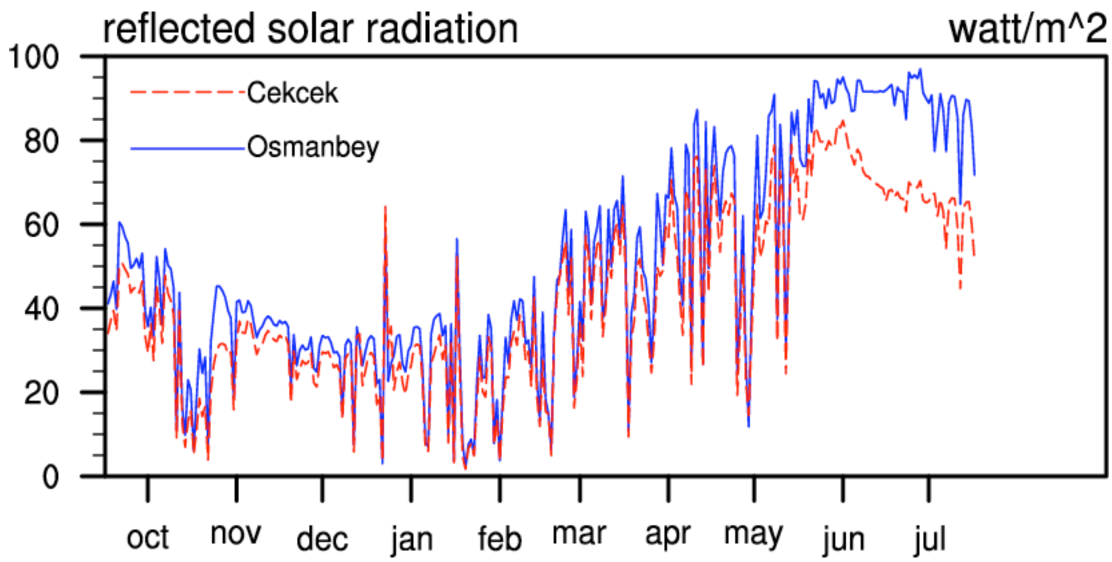

Figure.3.49 Model results for reflected solar radiation for Osmanbey and Çekçek

Absorbed solar radiation and its components, absorbed from ground and absorbed from the vegetation are shown in Figure.3.50, Figure.3.51 and Figure.3.52 respectively.

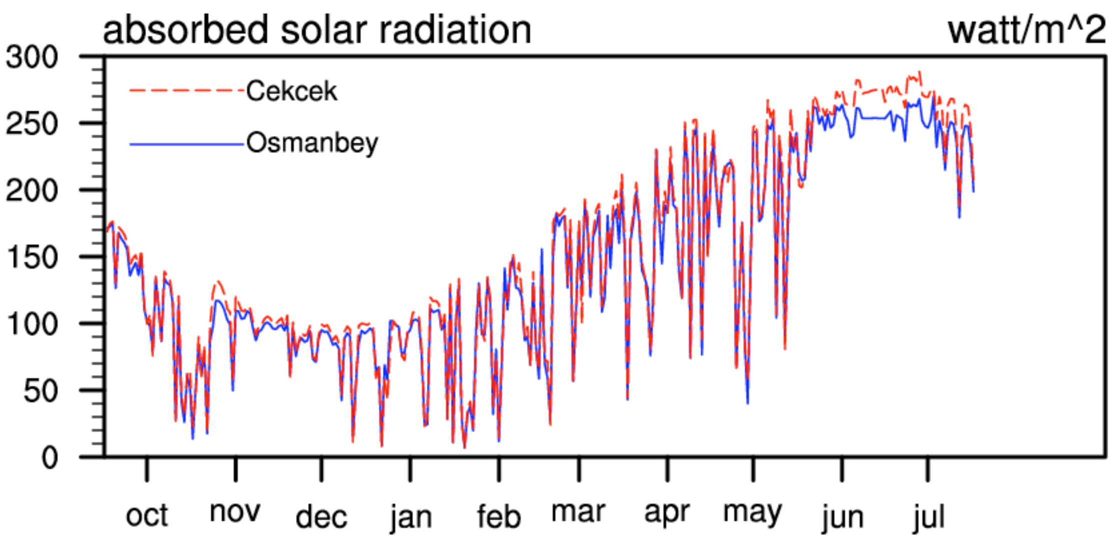

Figure.3.50 Model results for absorbed solar radiation for Osmanbey and Çekçek

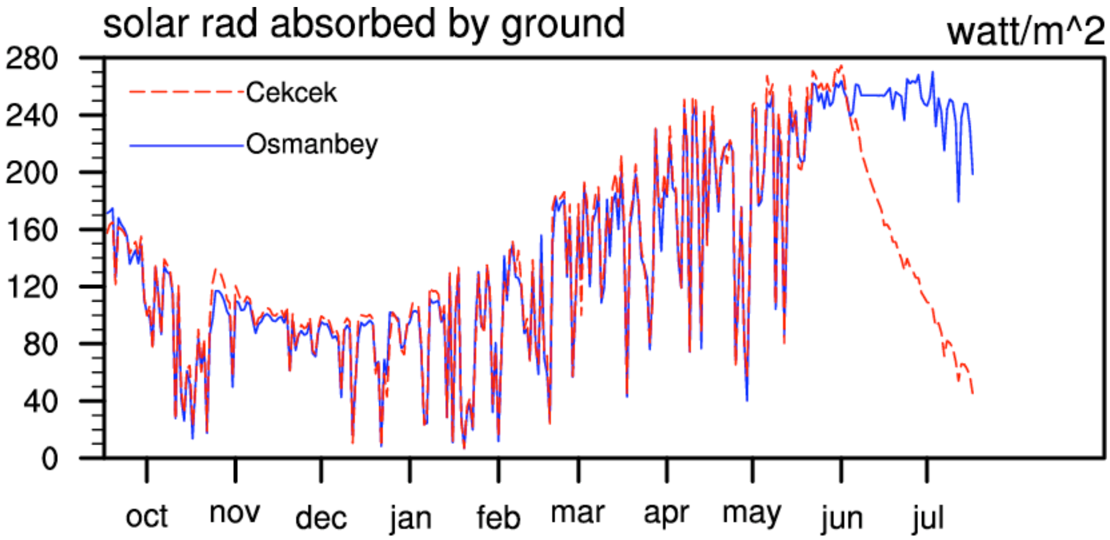

Figure. 3.51 Model results for solar radiation absorbed by ground for Osmanbey and Çekçek

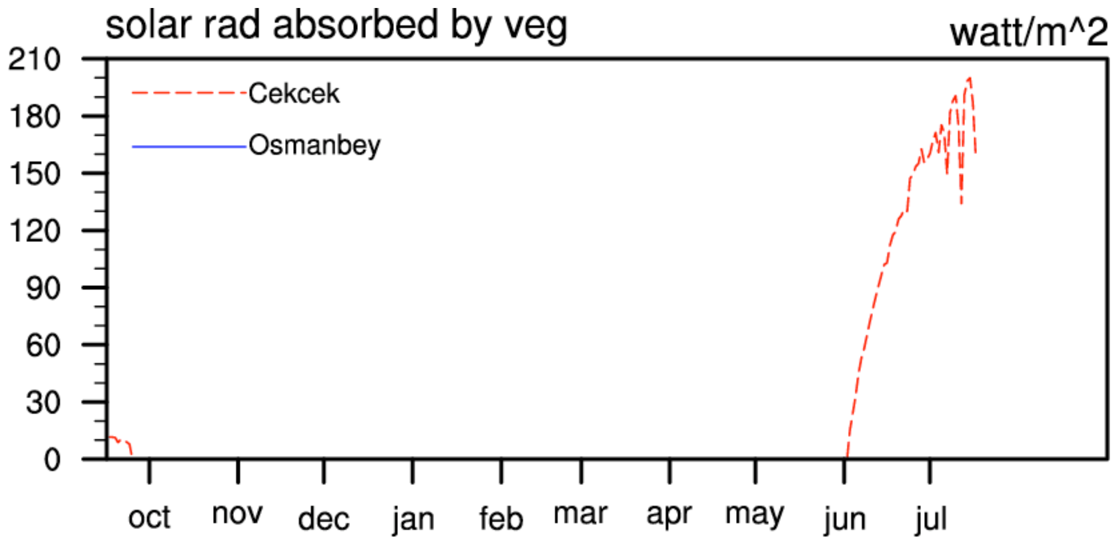

Figure3.52 Model results for solar radiation absorbed by vegetation for Osmanbey and Çekçek

After giving the solar radiation and its components, Figure.3.53 and Figure.3.54 show the infrared (longwave) radiation results. While the first one shows the net infrared values, the latter figure represents the emitted infrared radiation results.

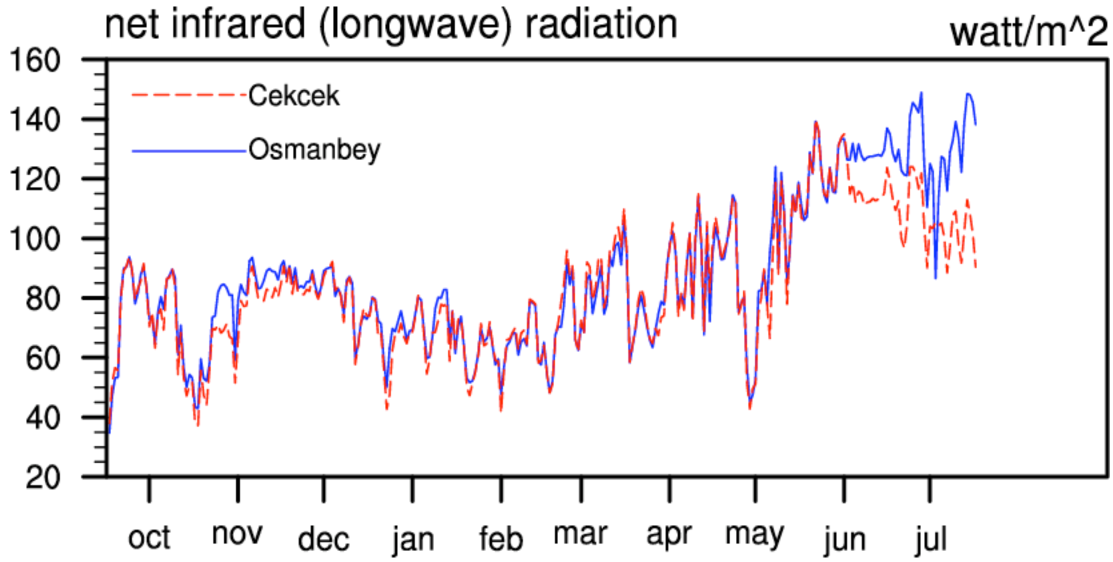

Figure.3.53 Model results for net infrared (longwave) radiation for Osmanbey and Çekçek

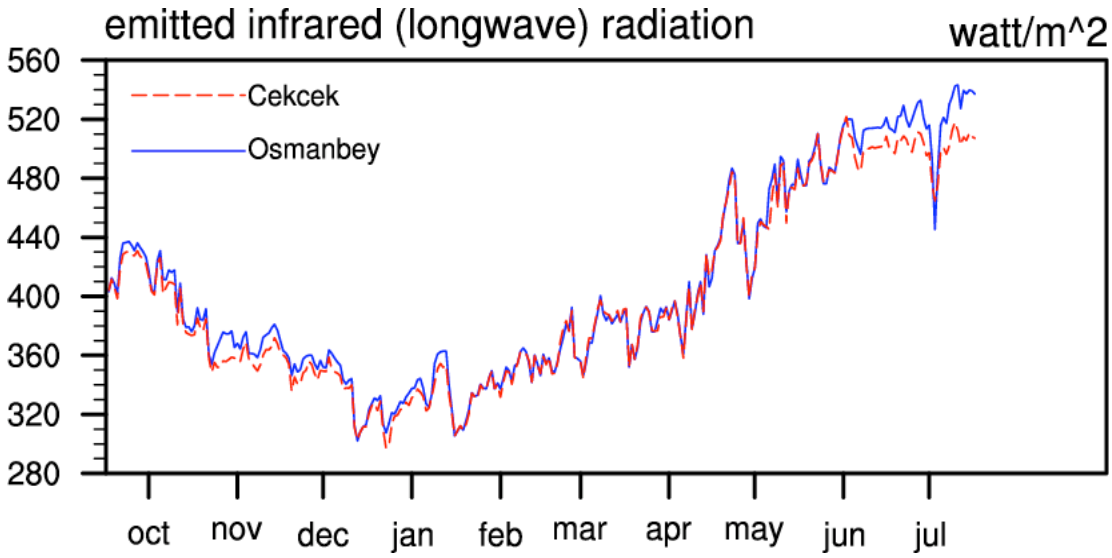

Figure.3.54 Model results for emitted infrared radiation for Osmanbey and Çekçek

4. CONCLUSIONS and DISCUSSIONS

4.1. Summary

As introduced in this paper, to describe the impact of irrigation from GAP on the climate of the region; observational experiments are performed over two sites in southeast Anatolia region from September 2006 to August 2007. Through analyzing several observed meteorological parameters and running a land surface model for pre-GAP and post-GAP areas, current dissimilarities are represented.

4.2. Discussions

From the observational results, some important ideas can be inferred. As it is clearly seen from the plots, most of the meteorological parameters show different patterns during the summer months. This is probably caused by the vegetation over land. In the Çekçek area, cotton is sown around March, the plants start to grow from May and the leaves cover the region until harvested around early September. The leaf area index (LAI) values for the cotton plants have maximum values at the summer months of June and July.

Although there is similar insolation values for both of the experimental sites (Figure3.2), the net radiation amount held at the surface is definitely higher in Çekçek site rather than Osmanbey (Figure.3.6). This is probably caused by the different albedo values in these areas. The vegetation cover over Çekçek area changes the land surface color and roughness values and so decreases the albedo. This leads to the result that more solar energy is absorbed by the ground and less is reflected back to the atmosphere (Figure.3.49 and Figure.3.50). More net radiation on Çekçek surface means more energy is available on the ground for heat fluxes. This energy is largely used for evaporation from the soil and for transpiration from the cotton plants.

If the temperature observations are examined for summer months, one important fact can be understood: vegetated area is cooler than the bare ground area (Figure.3.10) even though there is more energy piled up there. This incident can be explained by understanding the partitioning of net radiation into sensible and latent heat fluxes. The sensible heat flux plot shows that there are relatively similar values for Çekçek and Osmanbey all year until June (Figure.3.32). After June sensible heat flux declines in

Çekçek. This is not because there is less heat energy there. The main reason is that most of the energy is used for latent heat flux rather than sensible heat flux. Evapotranspiration cools the surface as the process removes large amounts of energy from the surface. And this is why there is a cooler air over Çekçek area during summer. This is also called the cooling impact of vegetation. The relative humidity plots also support this fact (Figure.3.14). The humidity in Çekçek is much higher than Osmanbey during June and July due to evapotranspiration activities of plants, in other words, latent heat fluxes produced by both plants and soil.

The vegetation cover over Çekçek area also affects the wind speed. As it is demonstrated in the wind speed plots (Figures 3.22, 3.23, 3.24 and 3.25), the wind is much stronger in Osmanbey during summer months. The plants must have a frictional effect over wind and thus decreasing the wind speed over Çekçek area.

The diurnal cycles of all these parameters in each season (Figures 3.28, 3.29, 3.30 and 3.31) give enough evidence to support these abovementioned discussions. There can't be seen any significant differences in autumn, winter and spring; while the summer panel shows all these described dissimilarities.

After scrutinizing the observational results of the experiment, modeling studies also has considerable outcomes over the region. The modeling result versus observational data comparison plots reveal the performance of CLM over the experimental area. The net radiation plots (Figures 3.35, 3.36, 3.39 and 3.40) show strong similarities for both Osmanbey and Çekçek. All year daily averaged oscillations and weekly plots make it clear that land surface modeling over south east Anatolia can be achieved successfully.

One important contrast that can be taken out from the model outputs is that the irrigation induced vegetation cover over south east Anatolia can not be modeled with the current CLM version 3.0 due to the lack of irrigated crop vegetation type in the model. Since there is no irrigated crop option in CLM, the model simulation is done with normal crop vegetation type. This leads to the result that soil moisture over the region decrease during the spring months and there is no enough soil moisture left for the plants in summer (Figures 3.47 and 3.48). This causes the plants to go under stress and response by decreasing their evapotranspirational activities. As it can be understood from the soil moisture plots, the insufficient water in the soil causes decrease in latent heat fluxes and therewithal an increase in sensible heat flux. This is the main reason that although the model simulations for net radiation show consistent results, the sensible heat flux simulations are somehow erroneous (Figure.3.44).

Other than this result, the reflected and absorbed radiation parameters show logical outputs. More heat is absorbed by plants in Çekçek during summer (Figure.3.52) and more is reflected from ground in Osmanbey (Figure.3.49).

4.3. General Conclusions

It is understood that, vegetation together with irrigation over the area creates a cooler environment and at the same time a more humid air. The main presumed differences are changes in albedo, surface roughness and evapotranspiration activities.

As another conclusion the modeling studies also revealed high performance on reflecting the observations and therefore past or future scenarios can be run with the necessary input parameters.

All these results signify that the irrigation induced crop cultivation over southeast Anatolia definitely changes the weather and climate. Despite the fact that only 20% of GAP is completed yet, these demonstrated results can signal the possible effects over vast areas in future.

REFERENCES

Adegoke, J., Pielke, R. Sr., Carleton, A. M., 2007. Observational and modeling studies of the impacts of agriculture-related land use change on planetary boundary layer processes in the central U.S. Agricultural and Forest Meteorology 142, 203-215.

Akuzum, T., Kodal, S., Cakmak, B., 1997. Irrigation management in GAP. Water Resour. Dev. 13 (4), 547–560.

Benli, B., Kodal, S., 2003. A non-linear model for farm optimization with adequate and limited water supplies: Application to the South-east Anatolian Project (GAP) Region. Agricultural Water Management 62(2003) 187-203.

Bonan, G.B., Oleson, K.W., Vertenstein, M., Levis, S., Zeng, X., Dai, Y., Dickinson, R.E., and Yang, Z.-L. 2002a. The land surface climatology of the Community Land Model coupled to the NCAR Community Climate Model. J. Climate 15: 3123-3149.

Bonan, G.B., Levis, S., Kergoat, L., and Oleson, K.W. 2002b. Landscapes as patches of plant functional types: An integrating concept for climate and ecosystem models. Global Biogeochem. Cycles 16: 5.1-5.23.

Cetin, O., Ozyurt, E., Sener, S., 1994. The effects of different irrigation methods on the yield and water use efficiency of cotton in Harran Plain. In: Proceedings of the 17th European Regional Conference on Efficient and Ecologically Sound Use of Irrigation Water with Special Reference to European Countries. Varna, Bulgaria, May 16–22. ICID.

Cetin, O., 1996. Water consumption of second crop corn in the Harran Plain. Research Institude of Sanlıurfa. General Publication No: 90, pp. 46.

Dağdelen, N., Yılmaz, E., Sezgin, F., Gürbüz, T., 2006. Water-yield relation and water use efficiency of cotton (Gossypium hirsutum L.) and second crop corn (Zea mays L.) in western Turkey. Agricultural Water Management 82 (2006) 63–85.

Hoffman, F., Vertenstein, M., Levis, S., Thornton, P., and Oleson, K. 2004. Community Land Model Version 3.0 (CLM3.0) Developer's Guide.

Komuscu, A.U., Erkan, A., Oz, S., 1998. Possible impacts of climate change on soil moisture availability in the Southeast Anatolia Development Project Region (GAP): An analysis from an agricultural drought perspective. Climatic Change 40, 3-4, pp 519-545.

Levis, S., Bonan, G.B., Vertenstein, M., and Oleson, K.W. 2004. The Community Land Model's Dynamic Global Vegetation Model (CLM-DGVM): Technical description and user's guide. NCAR Technical Note NCAR/TN-459+IA. National Center for Atmospheric Research, Boulder, CO.

Lioubimtseva, E., Cole, R., Adams, J.M., Kapustin, G., 2005. Impacts of climate and land-cover changes in arid lands of Central Asia. Journal of Arid Environments 62, 285-308.

Oleson,K.W., Dai, Y., Bonan, G., Bosilovich, M., Dickinson, R., Dirmeyer, P., Hoffman, F., Houser, P., Levis, S., Niu, G.Y., Thornton, P., Vertenstein, M., Yang, Z.L., Zeng, X. 2004. Technical Description of the Community Land Model (CLM).

Önol, B., 2001. Climate simulation of Turkey and its neighbourhood by regional climate model: Sensitivity of surface conditions, *M.Sc. Thesis,* Istanbul Technical University.

Raddatz, R.L., 2007. Evidence for the influence of agriculture on weather and climate through the transformation and management of vegetation: Illustrated by examples from the Canadian Prairies. Agricultural and Forest Meteorology 142, 186–202.

Sarkar, S., Chiu, L., Kafatos, M., Singh, R., 2007. Sensitivity of rainfall on land cover change over South East Asia: Some observational results. Advances in Space Research 39, 73-78.

T.C. Başbakanlık GAP Bölge Kalkınma İdaresi Başkanlığı. 2006.
http://www.gap.gov.tr/gap.php?sayfa=Turkish/Ggbilgi/gnedir.html.

USDA-FAS (United States Department of Agriculture, Foreign Agricultural Service).2007.
http://www.fas.usda.gov/remote/mideast_pecad/turkey/turkey.htm

Ünver, I.H.O. 1997. South-eastern Anatolia Integrated Development Project (GAP), Turkey: An Overview of Issues of Sustainability. Water Resources Development, Vol. 13, No. 2, pp.187-207.

Vertenstein, M., Hoffman, F., Oleson, K., and Levis, S. 2004. Community Land Model Version 3.0 (CLM3.0) User's Guide.

Yazar, A., Sezen, S.M., Gencel, B., 2002a. Drip irrigation of corn in the Southeast Anatolia Project (GAP) area in Turkey. Irrig. Drain. 51, 293–300.

Yazar, A., Sezen, S.M., Sesveren, S., 2002b. LEPA and trickle irrigation of cotton in the Southeast Anatolia Project (GAP) area in Turkey. Agric. Water Manag. 54, 189-203.

Zeng, X. 2001. Global vegetation root distribution for land modeling. J. Hydrometeor. 2:525-530.

APPENDIX – CLM MODEL EQUATIONS

Surface energy and water balance equations:

$$R_n = G + H + \lambda E$$

R_n is net radiaton, G is ground heat flux, H is sensible heat flux and λE is latent heat flux.

$R_n = S\downarrow (1-\alpha) + L\downarrow - L\uparrow$

$L\uparrow = \varepsilon\sigma T^4$

$RunOff = P - E - I$

P is precipitation and E is evaporation.

Radiative Transfer equations:

$$-\bar{\mu}\frac{dI\uparrow}{d(L+S)} + \left[1-(1-\beta)\omega\right]I\uparrow - \omega\beta I\downarrow = \omega\bar{\mu}K\beta_0 e^{-K(L+S)}$$

$$\bar{\mu}\frac{dI\downarrow}{d(L+S)} + \left[1-(1-\beta)\omega\right]I\downarrow - \omega\beta I\uparrow = \omega\bar{\mu}K(1-\beta_0)e^{-K(L+S)}$$

I is diffuse radiative flux, *K* is optical depth of direct beam per unit of leaf stem area, *u* is cosine of zenith anfgle of incident beam, *B* is upscatter parameter for diffuse and direct beam. *W* is scattering coefficient, *L* is exposed leaf area index and *S* is exposed stem area index.

Momentum, Sensible Heat and Laten Heat Fluxes:

τ_x and τ_y are momentum fluxes

$$\tau_x = -\rho_{atm}\frac{(u_{atm} - u_s)}{r_{am}}$$

$$\tau_y = -\rho_{atm}\frac{(v_{atm} - v_s)}{r_{am}}$$

H is sensible heat flux

$$H = -\rho_{atm}C_p\frac{(\theta_{atm} - \theta_s)}{r_{ah}}$$

E is water vapor flux

$$E = -\rho_{atm}\frac{(q_{atm} - q_s)}{r_{aw}}.$$

VITA

Altuğ Ekici was born in 23.04.1983 in İskenderun/Hatay. He completed his primary education in İskenderun and then attended to Adana Science High School for the first two years of his secondary education. After graduating from Gündoğdu College in Adana, he enrolled at Sabanci University Faculty of Engineering and Natural Sciences in 2001. Completing his undergraduate study and achieving the degree of Bachelor of Science in Computer Science and Engineering in 2006, he started his graduate education in Eurasia Institute of Earth Sciences in İstanbul Technical University. He is currently enrolled to Earth System Sciences Master program in this institute.